

# Electronic Supplementary Information

## Water Molecular Bridge-Induced Selective Dual Polarization in Crystals for Stable Multi-Emitter

Yi Xing,<sup>[a]</sup> Zhongyu Li,<sup>[a]</sup> Glib V. Baryshnikov,<sup>[b]</sup> Shen Shen,<sup>[a]</sup> Danfeng Ye,<sup>[a]</sup> Hans Ågren,<sup>[c]</sup> Liangliang Zhu\*<sup>[a]</sup>

[a] State Key Laboratory of Molecular Engineering of Polymers, Department of Macromolecular Science, Fudan University, Shanghai 200438, China. E-mail: zhuliangliang@fudan.edu.cn

[b] Laboratory of Organic Electronics, Department of Science and Technology, Linköping University, 60174 Norrköping, Sweden

[c] Department of Physics and Astronomy, Uppsala University, Box 516, SE-751 20 Uppsala, Sweden

## Content

1.Materials and methods .....	3
2.Synthesis and characterization of compounds .....	5
3.Additional luminescent, thermal and structural properties. ....	9
4.Characterization spectra. ....	16
5.Single crystal analysis of compounds .....	26
6.Reference .....	30

## 1. Materials and methods

### Materials and measurements

All reagents were purchased from commercial sources without further purification. Deuterated solvents were purchased from Cambridge Isotope Laboratory (Andover, MA). The  $^1\text{H}$  NMR and  $^{19}\text{F}$  NMR were measured on a Bruker 400L spectrometer in chloroform- $d$  and DMSO- $d_6$  using tetramethylsilane as internal standard. Mass spectra were recorded on a Matrix Assisted Laser Desorption Ionization-Time of Flight/Time of Flight (MALDI-TOF) Mass Spectrometer (5800). Photoluminescence (PL) spectra were collected on an Edinburgh FLS-1000 luminescence spectrometer equipped with a xenon lamp. The PL decay spectra were recorded on Edinburgh FLS-1000 luminescence spectrometer equipped with a microsecond flashlamp as the excitation source (frequency = 100 Hz) and EPL-375 nm, EPL-510 nm, EPL-450 nm picosecond pulsed diode laser as the excitation source for microsecond and time correlated single-photon counting (TCSPC) measurements, respectively. Single crystal X-ray diffraction signals were collected by a Bruker D8 Venture operating at room temperature, and their structures were resolved and analyzed with the assistance of shelx-2014 software. Optical fluorescence images were taken by using a Nikon microscope with the excitation of UV (365 nm) light. WAXS data were collected by Xenocs Xeuss2.0. TGA was achieved using Mettler Toledo TGA 1. Perkin-Elmer Lambda750 was used to collect UV-Vis data.

### Preparation and measurement steps

**Solution:** DPP-F (53.2 mg) was dissolved in DMF/DMSO/ACN/Acetone/1,4-dioxane/EA/THF/DCM solvents (20 mL) to make a solution of  $1 \times 10^{-5}$  mol/L. DPP and PP-F solutions were also prepared with the same concentration. These solutions were then used for UV-Vis measurement, while DMF solutions of  $1 \times 10^{-4}$  mol/L of the three compounds were prepared for photoluminescence (PL) study. Water was mixed into a DMSO solution of DPP-F with different volume ratios to maintain a final concentration of  $1 \times 10^{-4}$  mol/L to study the aggregation states of the solution by PL spectroscopy.

**Crystal:** The single crystals were cultivated by recrystallization. The three compounds were dissolved by ordinary ethanol without further drying, stirred and heated until completely dissolved, and then cooled until crystallization. Loaded crystals with fluted solid cuvettes without damaging were placed on FLS 1000 spectrometer to collect PL spectra.

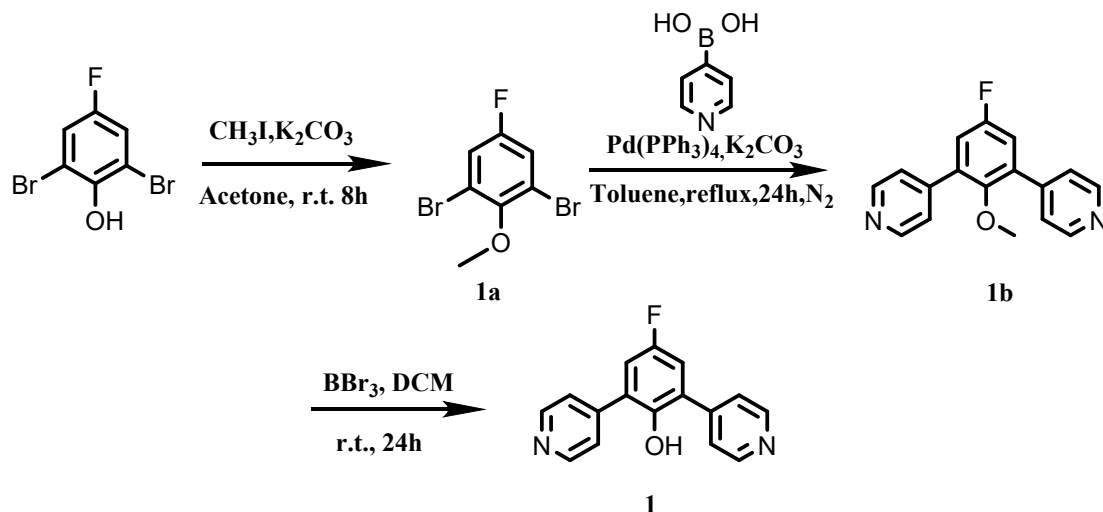
### Theoretical calculation

The calculated dipole moments  $\mu$  of the ground state geometries for a) single molecule and b) crystal structures at B3LYP/6-31G(d, p) level using Gaussian 09 package. The model for calculating dipole moments were selected with four molecules and four water, which simulated the periodic arrangement of crystals with the smallest repeating unit. This model is close to the real molecular arrangement of the crystals to the most extend with minimum conformational deformation upon optimization. Molecular geometry optimization was carried out at the DFT level by using the B3LYP exchange-correlation functional<sup>[1]</sup> and 6-31+G(d) basis set.<sup>[2]</sup> Grimme's empirical dispersion correction (GD3)<sup>[3]</sup> was employed in all performed calculations. Excited state calculations (vertical absorption and emission singlet-singlet transitions as well as excited states

optimization) were performed by TDDFT method<sup>[4]</sup> using GD3-B3LYP/6-31+G(d) approach. For accounting of the solvent effect on the excited state energy the polarizable continuum model (PCM)<sup>[5]</sup> was used (model solvent – DMF). <sup>[5]</sup> All the calculations were carried out using the Gaussian 16 (Revision C.01) program package.<sup>[6]</sup>

## 2.Synthesis and characterization of compounds

**Scheme S1.** Synthesis of DPP-F

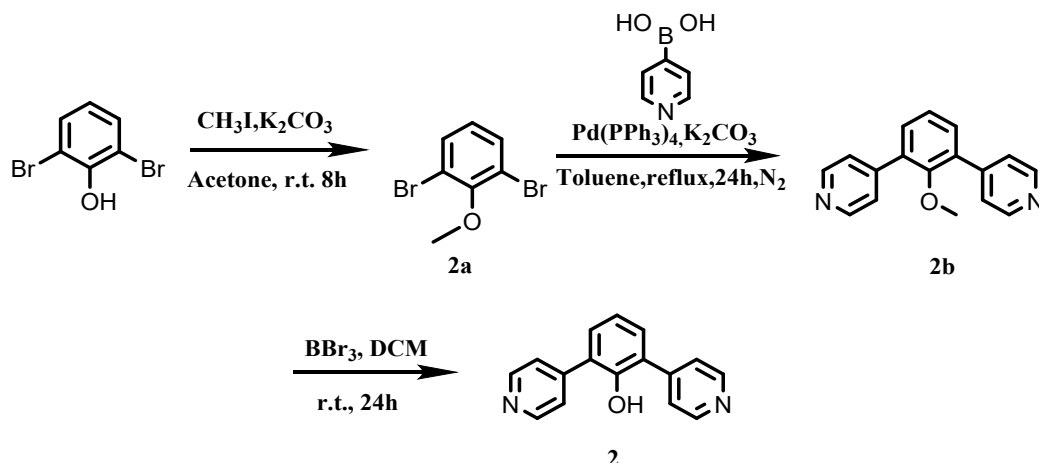


**The synthesis of 1a.** 2,6-Dibromo-4-fluorophenol (2.7 g, 10 mmol) and  $\text{K}_2\text{CO}_3$  (2.76 g, 20 mmol) was dropped into a 100 mL round bottle flask, then, 50 mL acetone and iodomethane (2.8 g, 1.25 mL, 20 mmol) was also injected into the system, the reaction was carried under room temperature for 5 hours. The solvent was removed under reduce pressure and purified by solution extraction ( $\text{H}_2\text{O}/\text{DCM}$ ), 2.43 g compounds was obtained, yield = 90 %,  $^1\text{H}$  NMR (400 MHz, DMSO)  $\delta$  7.70 (d,  $J$  = 8.0 Hz, 2H), 3.77 (s, 3H).  $^{19}\text{F}$  NMR (376 MHz, DMSO)  $\delta$  -114.96.  $^{13}\text{C}$  NMR (101 MHz,  $\text{CDCl}_3$ )  $\delta$  159.40, 156.91, 151.12, 119.92, 119.67, 118.10, 117.99, 60.76.

**The synthesis of 1b.** **1a** (1.42 g, 5 mmol), pyridin-4-yl boronic acid (1.85 g, 15 mmol), and  $\text{Pd}(\text{PPh}_3)_4$  (577 mg, 0.5 mmol),  $\text{K}_2\text{CO}_3$  (2.76 g, 20 mmol) were dissolved in a mixture of DMF (50 mL) /  $\text{H}_2\text{O}$  (2 mL). The mixture was stirred at 110 °C for 24 h under nitrogen. After cooling to room temperature, the mixture was poured into water (200 mL) and extracted three times with  $\text{CH}_2\text{Cl}_2$ . The organic layer was dried over anhydrous  $\text{Na}_2\text{SO}_4$ . After removing the solvent under reduced pressure, the residue was chromatographed on a silica gel column with  $\text{DCM}/\text{MeOH}$  (80:1, v/v), 712 mg **1b** was obtained, Yield: 50%.  $^1\text{H}$  NMR (400 MHz,  $\text{CDCl}_3$ )  $\delta$  8.75 (d,  $J$  = 6.2 Hz, 4H), 7.63 (d,  $J$  = 6.2 Hz, 4H), 7.20 (d,  $J$  = 8.4 Hz, 2H), 3.18 (s, 3H).  $^{19}\text{F}$  NMR (376 MHz,  $\text{CDCl}_3$ )  $\delta$  -116.59.  $^{13}\text{C}$  NMR (101 MHz,  $\text{CDCl}_3$ )  $\delta$  151.34, 150.67, 150.10, 149.97, 144.98, 134.75, 133.98, 130.76, 130.50, 128.40, 127.97, 124.39, 123.82, 117.57, 117.34, 61.24.

**The synthesis of DPP-F. 1b** (556 mg, 2 mmol) was dissolved into 30 mL fresh distilled  $\text{DCM}$  in a 100 mL schlenk flask, then 10 mL 1M  $\text{DCM}$  solution of  $\text{BBr}_3$  was dropped slowly into the system, the solution was stirred overnight. 100 mL 10%  $\text{NaHCO}_3$  aqueous solution was added into the resulting solution. Then the mixture was neutralized to pH = 8~9, the precipitated was collected and further purified by column ( $\text{DCM}/\text{MeOH}$  : v/v = 40/1). A light pink powder (178 mg) was obtained, yield = 33%.  $^1\text{H}$  NMR (400 MHz,  $\text{CDCl}_3$ )  $\delta$  8.64 (d,  $J$  = 6.1 Hz, 4H), 7.48 (d,  $J$  = 6.1 Hz, 4H), 7.08 (d,  $J$  = 8.4 Hz, 2H).  $^{19}\text{F}$  NMR (376 MHz, DMSO)  $\delta$  -114.98.  $^{13}\text{C}$  NMR (101 MHz,  $\text{CDCl}_3$ )  $\delta$  158.07, 155.67, 149.51, 146.58, 145.57, 128.73, 128.66, 124.24, 117.28, 117.05.

**Scheme S2. Synthesis of DPP**

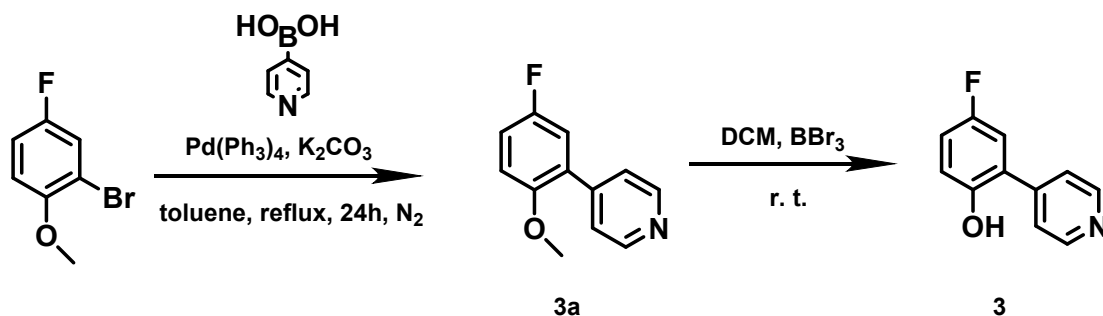


**The synthesis of 2a.** As mentioned in our previous work<sup>11</sup>, 2,6-dibromophenol (2.52 g, 10 mmol) and  $K_2CO_3$  (2.76 g, 20 mmol) was dropped into a 100 mL round bottle flask, then, 50 mL acetone and iodomethane (2.8 g, 1.25 mL, 20 mmol) was also injected into the system, the reaction was carried under room temperature for 5 hours. The solvent was removed under reduce pressure and purified by solution extraction ( $H_2O$ /DCM), 2.47 g clear liquid was obtained, yield = 93%,  $^1H$  NMR (400 MHz,  $CDCl_3$ )  $\delta$  7.49 (d,  $J$  = 8.0 Hz, 2H), 6.86 (t,  $J$  = 8.0 Hz, 1H), 3.89 (s, 3H).  $^{13}C$  NMR (101 MHz,  $CDCl_3$ )  $\delta$  154.35 (s), 132.83 (s), 126.44 (s), 118.45 (s), 60.71 (s).

**The synthesis of 2b.** **2a** (1.33 g, 5 mmol), pyridin-4-yl boronic acid (1.85 g, 15 mmol), and  $Pd(PPh_3)_4$  (577 mg, 0.5 mmol),  $K_2CO_3$  (2.76 g, 20 mmol) were dissolved in a mixture of DMF (50 mL) /  $H_2O$  (2 mL). The mixture was stirred at 110 °C for 24 h under nitrogen. After cooling to room temperature, the mixture was poured into water (200 mL) and extracted three times with  $CH_2Cl_2$ . The organic layer was dried over anhydrous  $Na_2SO_4$ . After removing the solvent under reduced pressure, the residue was chromatographed on a silica gel column with DCM/MeOH (80:1, v/v), 773 mg white solid **3b** was obtained, Yield: 59%.  $^1H$  NMR (400 MHz,  $CDCl_3$ )  $\delta$  8.70 (dd,  $J$  = 4.5, 1.6 Hz, 4H), 7.54 (dd,  $J$  = 4.5, 1.7 Hz, 4H), 7.45 (t,  $J$  = 1.5 Hz, 1H), 7.22 (d,  $J$  = 1.5 Hz, 2H), 3.95 (s, 3H).  $^{13}C$  NMR (101 MHz,  $CDCl_3$ )  $\delta$  149.98, 146.05, 133.39, 131.34, 125.09, 124.10, 61.18.

**The synthesis of DPP.** **2b** (524 mg, 2 mmol) was dissolved into 30 mL fresh distilled DCM in a 100 mL schlenk flask, the system was cooling down to 0 °C by a mixture of ice and water, then 10 mL 1M DCM solution of  $BBr_3$  was dropped slowly into the system, the solution was stirred for 5 min and then allowed to worm to room temperature and further stirred overnight, under argon atmosphere. 100 mL 10%  $NaHCO_3$  aqueous solution was added into the resulting solution. Then the mixture was neutralized to pH = 8~9, and the precipitated was collected and further purified by column (DCM/MeOH : v/v = 50/1). A light pink powder (228 mg) was obtained, yield = 46%.  $^1H$  NMR (400 MHz, DMSO)  $\delta$  8.98 (s, 1H), 8.63 (d,  $J$  = 5.9 Hz, 4H), 7.58 (d,  $J$  = 6.0 Hz, 4H), 7.39 (d,  $J$  = 7.6 Hz, 2H), 7.14 (t,  $J$  = 7.6 Hz, 1H).  $^{13}C$  NMR (101 MHz, DMSO)  $\delta$  150.92, 149.51, 146.00, 130.89, 128.79, 124.24, 121.25.

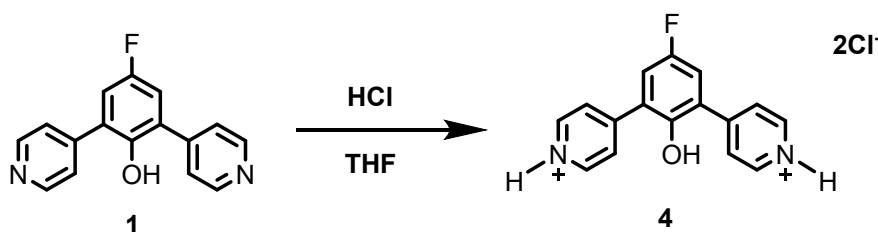
Scheme S3. Synthesis of PP-F



**The synthesis of 3a.** 2-Bromo-4-fluoroanisole (1.025 g, 5 mmol), pyridin-4-yl boronic acid (1.85 g, 15 mmol), and  $\text{Pd(PPh}_3)_4$  (577 mg, 0.5 mmol),  $\text{K}_2\text{CO}_3$  (2.76 g, 20 mmol) were dissolved in a mixture of DMF (50 mL) /  $\text{H}_2\text{O}$  (2 mL). The mixture was stirred at 110 °C for 48 h under nitrogen. After cooling to room temperature, the mixture was poured into water (200 mL) and extracted three times with  $\text{CH}_2\text{Cl}_2$ . The organic layer was dried over anhydrous  $\text{Na}_2\text{SO}_4$ . After removing the solvent under reduced pressure, the residue was chromatographed on a silica gel column with DCM/ MeOH (80:1, v/v), 568 mg **3a** was obtained, Yield: 56 %.  $^1\text{H}$  NMR (400 MHz,  $\text{CDCl}_3$ )  $\delta$  8.68 – 8.59 (m, 1H), 7.49 – 7.42 (m, 1H), 7.12 – 7.03 (m, 1H), 6.94 (dd,  $J$  = 9.9, 4.4 Hz, 1H), 3.81 (s, 2H).  $^{19}\text{F}$  NMR (376 MHz,  $\text{CDCl}_3$ )  $\delta$  -123.36.  $^{13}\text{C}$  NMR (101 MHz,  $\text{CDCl}_3$ )  $\delta$  158.32, 155.94, 152.77, 149.38, 145.46, 124.17, 117.16, 116.92, 116.15, 115.93, 112.66, 112.58, 56.19.

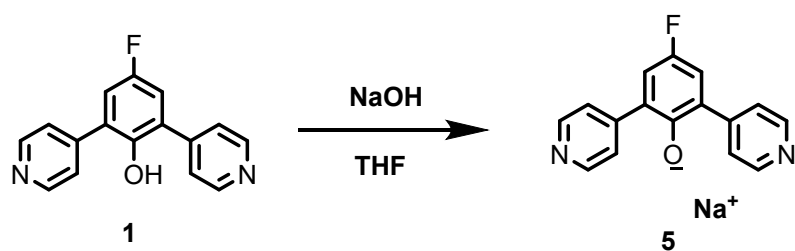
**The synthesis of PP-F.** **3a** (406 mg, 2 mmol) was dissolved into 30 mL fresh distilled DCM in a 100 mL schlenk flask, the system was cooling down to 0 °C by a mixture of ice and water, then 10 mL 1M DCM solution of  $\text{BBr}_3$  was dropped slowly into the system, the solution was stirred for 5 min and then rest to room temperature and further stirred overnight, under argon atmosphere. 100 mL 10%  $\text{NaHCO}_3$  aqueous solution was added into the resulting solution. Then the mixture was neutralized to pH = 8~9, and the precipitated was collected and further purified by column (DCM/MeOH : v/v = 40/1). A white powder (174 mg) was obtained, yield = 46%.  $^1\text{H}$  NMR (400 MHz,  $\text{CDCl}_3$ )  $\delta$  8.67 – 8.63 (m, 2H), 7.58 – 7.54 (m, 2H), 7.07 – 6.97 (m, 2H), 6.95 – 6.90 (m, 1H).  $^{19}\text{F}$  NMR (376 MHz,  $\text{CDCl}_3$ )  $\delta$  -123.64.  $^{13}\text{C}$  NMR (101 MHz, DMSO)  $\delta$  157.30, 154.97, 149.90, 145.21, 125.99, 125.91, 124.18, 117.84, 117.76, 116.89, 116.67, 116.58, 116.35.

Scheme S4. Synthesis of the protonated species



**The synthesis of the protonated species.** **1** (532 mg, 2 mmol) was dissolved into 30 mL THF with dilute hydrochloric acid, and the system was stirred for 0.5 h. After removing the solvent under reduced pressure, the protonated species was obtained for 641 mg.  $^1\text{H}$  NMR (400 MHz, DMSO)  $\delta$  9.08 – 9.01 (m, 4H), 8.34 (ddq,  $J$  = 4.5, 2.2, 1.1 Hz, 4H), 7.70 (d,  $J$  = 8.8 Hz, 2H).

**Scheme S5.** Synthesis of the deprotonated species



**The synthesis of the deprotonated species.** **1** (532 mg, 2 mmol) was dissolved into 30 mL THF. 320 mg (8 mmol) NaOH was then added into the solution, and the system was stirred for 2 h. After filtering out the solid and removing the solvent under reduced pressure, the deprotonated species was obtained for 545 mg. <sup>1</sup>H NMR (400 MHz, DMSO)  $\delta$  8.50 – 8.34 (m, 4H), 7.86 (d,  $J$  = 5.5 Hz, 4H), 7.21 – 7.08 (m, 2H).



### 3. Additional luminescent, thermal and structural properties.

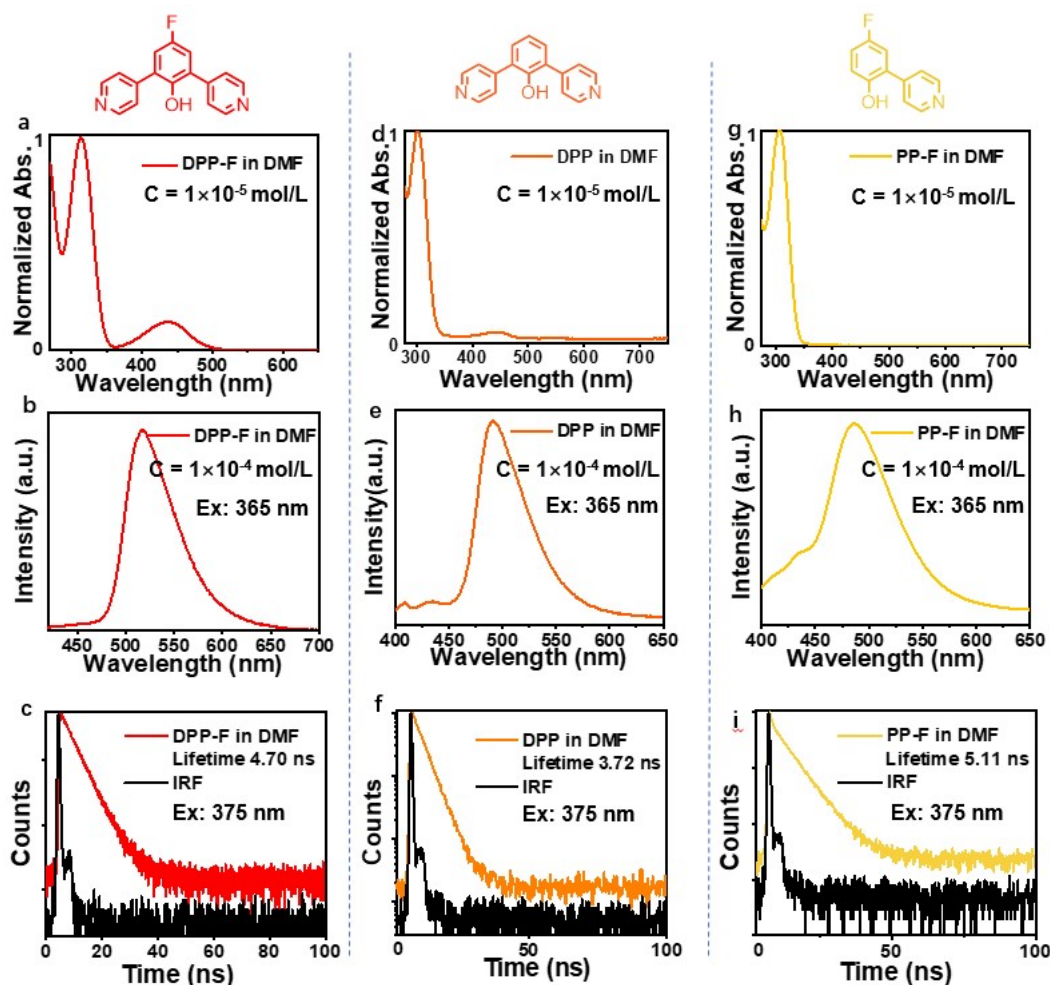


Figure S1. a, d, g) UV-Vis spectra of DPP-F, DPP and PP-F in DMF solution. b, e, h) Emission spectra of DPP-F, DPP and PP-F in DMF solution, respectively. c, f, i) Photoluminescence lifetime of DPP-F, DPP and PP-F in DMF solution, respectively.

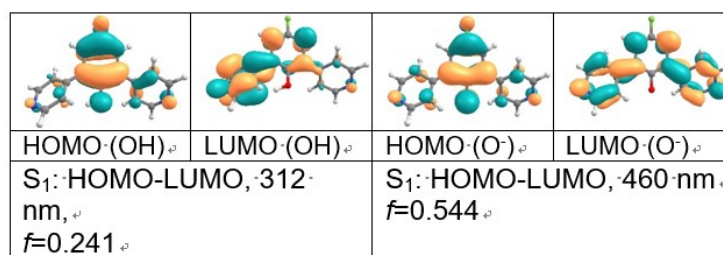


Figure S2. Selected molecular orbitals that are involved into the most important electronic transitions of neutral (OH) and anionic (O $^-$ ) forms of DPP-F.

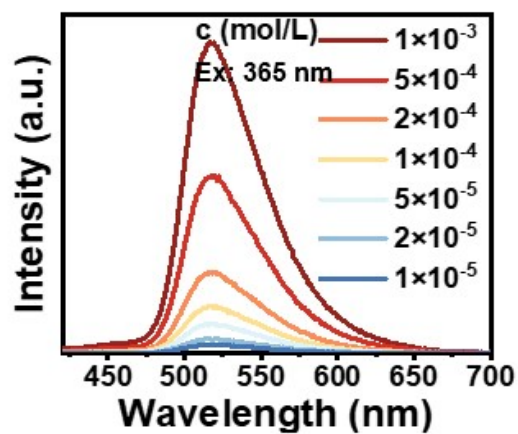


Figure S3. Emission spectrum of DPP-F at different concentration gradients in DMF.

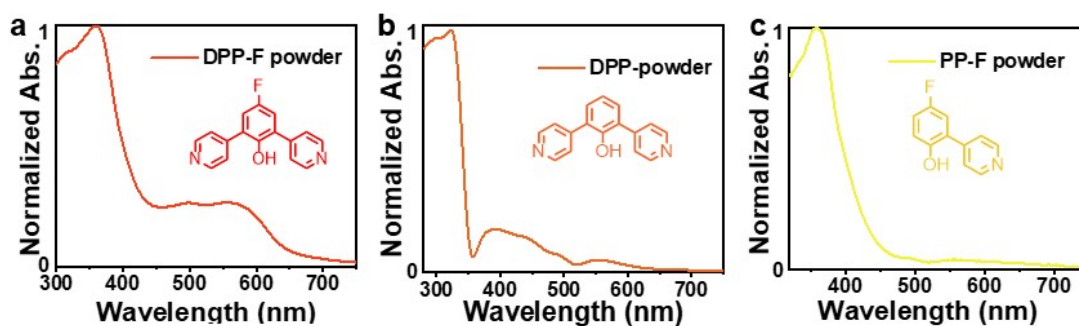


Figure S4. Absorption spectra of a) DPP-F powder, b) DPP powder and c) PP-F powder.

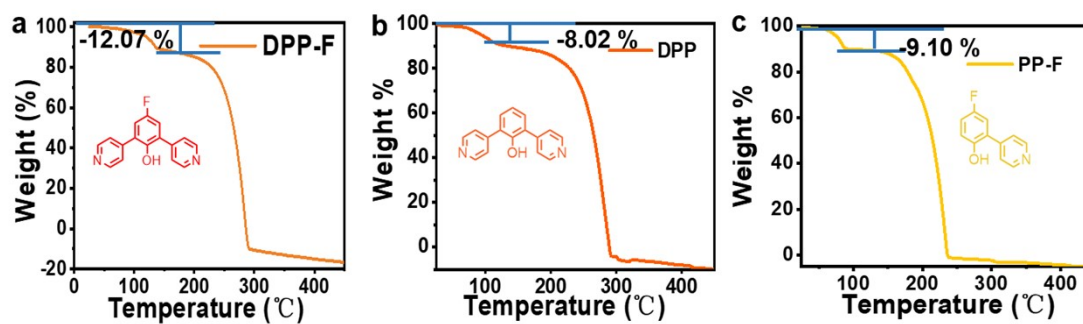


Figure S5. TGA thermograms of the crystal form of a) DPP-F, b) DPP, and c) PP-F.

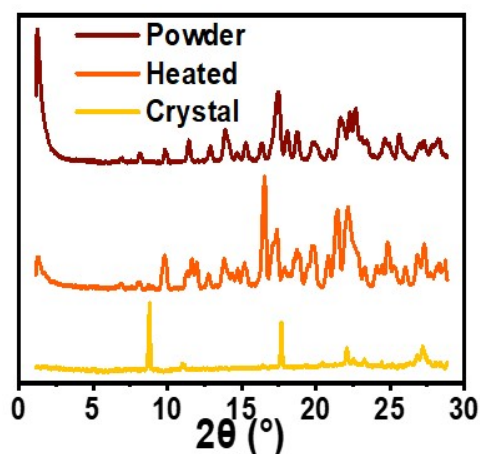


Figure S6. XRD pattern of the DPP-F powder, the dehydrated DPP-F powder from its crystal, and the DPP-F crystal.

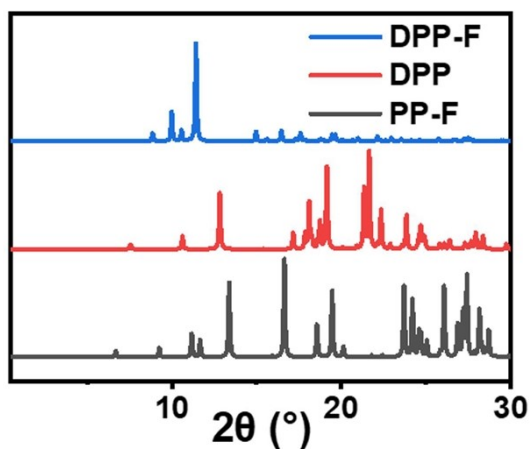


Figure S7. Simulated XRD crystal pattern of the three compounds.

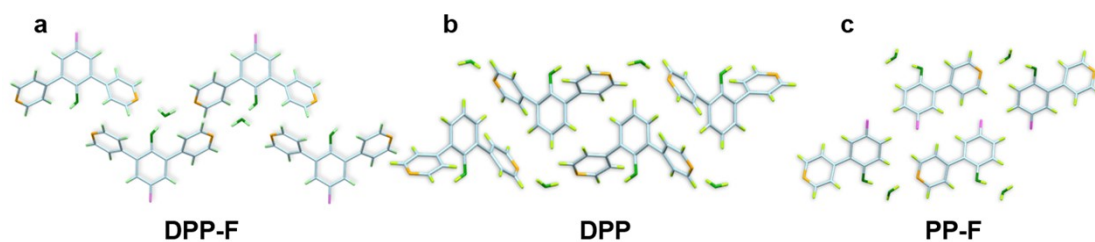


Figure S8. Crystal packing of a) DPP-F, b) DPP and c) PP-F.

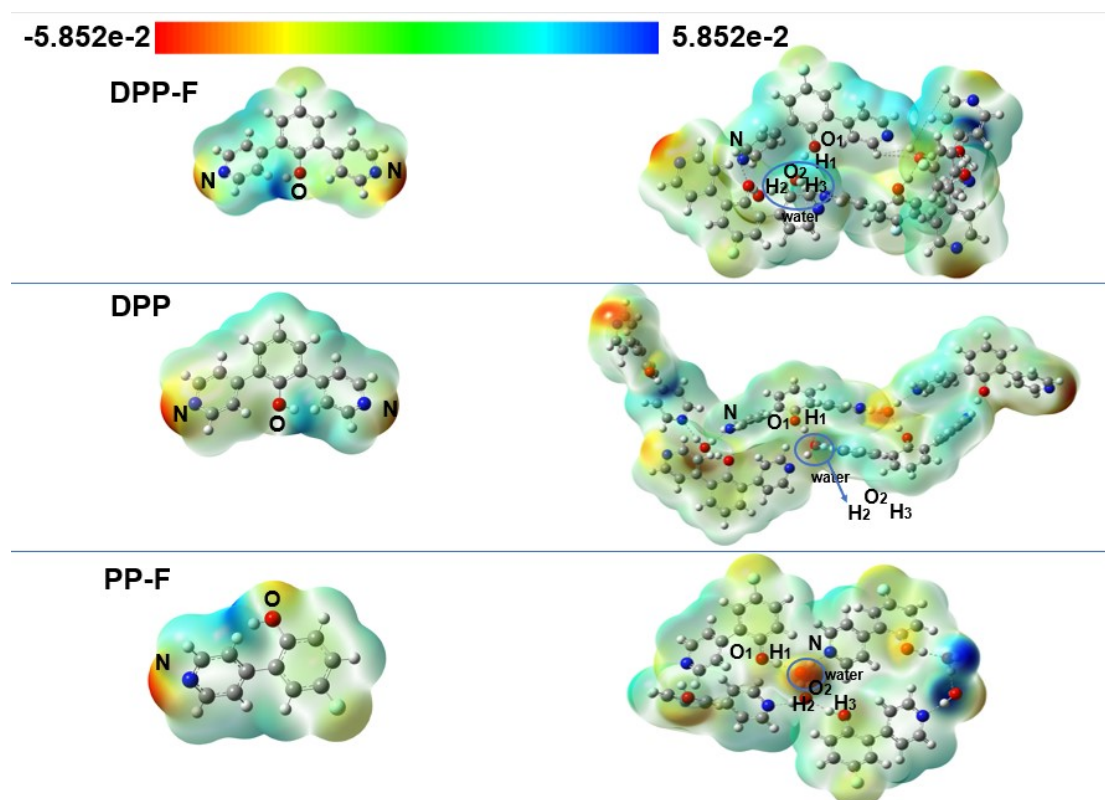


Figure S9. Electrostatic potential surfaces of DPP-F, DPP and PP-F.

Table S1. The Mulliken-charge value of key atoms (the number of atoms is consistent with Figure S9).

DPP-F Monomer	DPP-F Crystal	DPP Monomer	DPP Crystal	PP-F Monomer	PP-F Crystal
N: -0.43	N: -0.52	N: -0.42	N: -0.49	N: -0.42	N: -0.51
O: -0.56	O1: -0.62	O: -0.56	O1: -0.64	O: -0.56	O1: -0.62
N: -0.42	H1: 0.37	N: -0.43	H1: 0.39		H1: 0.37
	O2: -0.69(H <sub>2</sub> O)		O2: -0.70(H <sub>2</sub> O)		O2: -0.69(H <sub>2</sub> O)
	H2: 0.34(H <sub>2</sub> O)		H2: 0.34(H <sub>2</sub> O)		H2: 0.32(H <sub>2</sub> O)
	H3: 0.32(H <sub>2</sub> O)		H3: 0.34(H <sub>2</sub> O)		H3: 0.35(H <sub>2</sub> O)

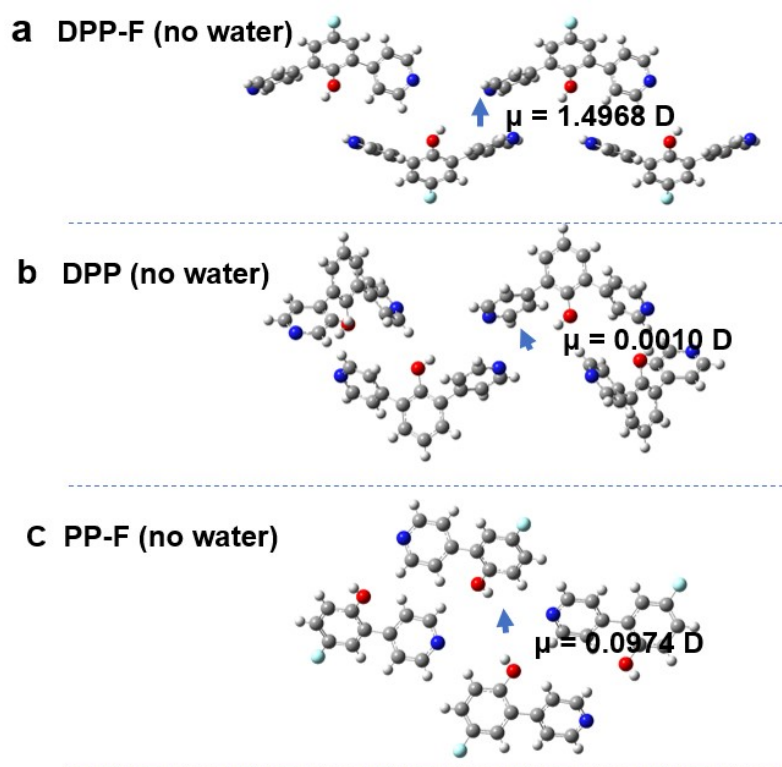


Figure S10. Calculated dipole moments of the three compounds after water removal.

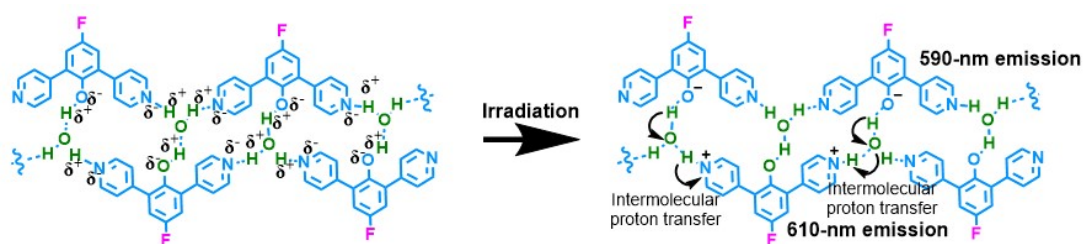


Figure S11. Proposed excited-state intermolecular proton transfer process assisted by water molecular bridge owe to the favorable distance of the intermolecular H-bonds.

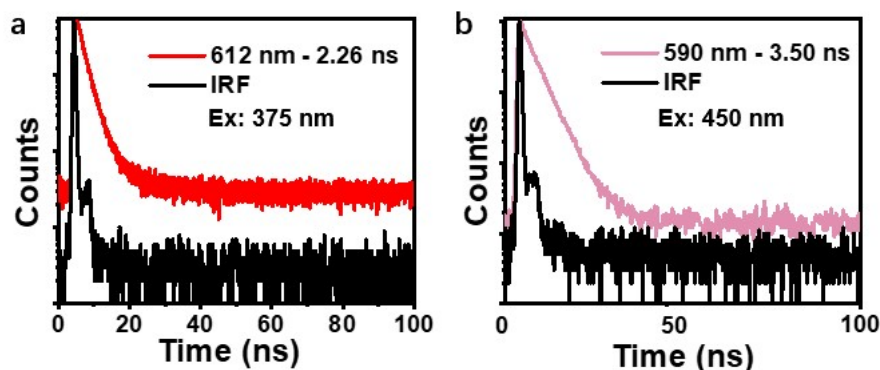


Figure S12. Photoluminescence lifetime of DPP-F crystal collected from the emission of a) 612 nm excited by 375 nm laser power and b) 590 nm excited by 450 nm laser power.



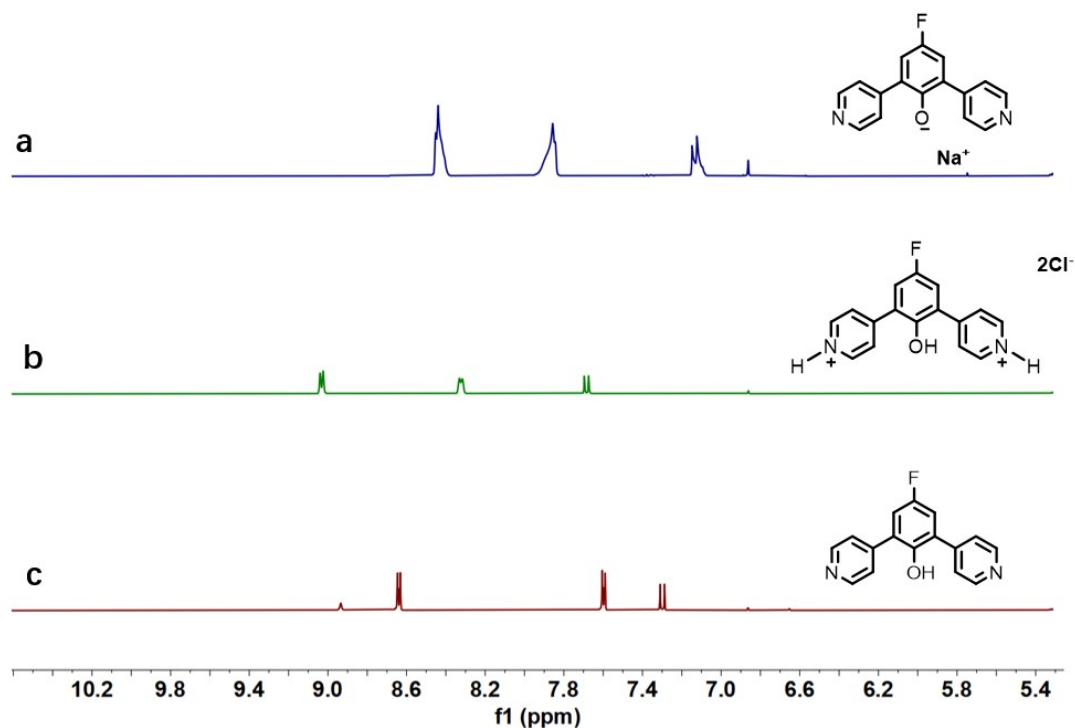


Figure S13.  $^1\text{H}$  NMR spectra of a) a fully deprotonated (reacted with NaOH) compound from DPP-F, b) a fully protonated (reacted with HCl) compound from DPP-F, and c) DPP-F.

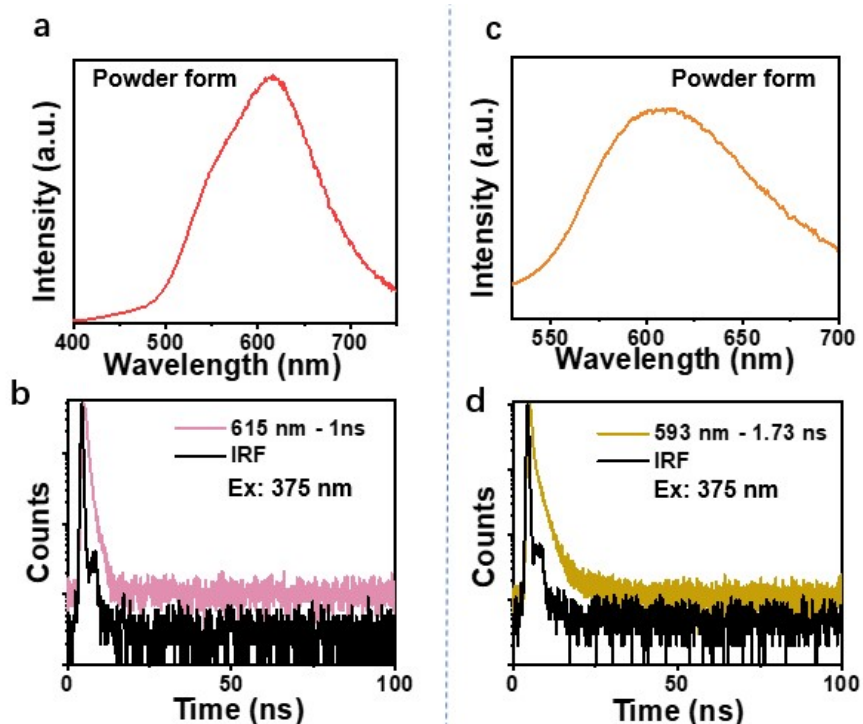


Figure S14. Emission spectra of a) the fully protonated compound in powder form and c) the fully deprotonated compound in powder form with their photoluminescence lifetime showing in b, d).

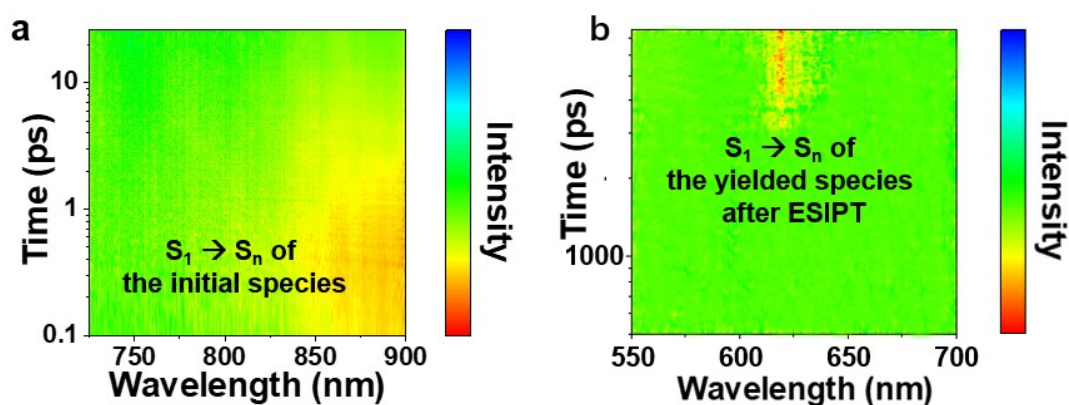


Figure S15. a) The three-dimensional transient absorption spectra mapping showing the excited-state absorption signal a) without and b) with thousands of picoseconds' pump-probe delay time, featuring the initial species and the yielded species after an excited-state intermolecular proton transfer process, respectively.

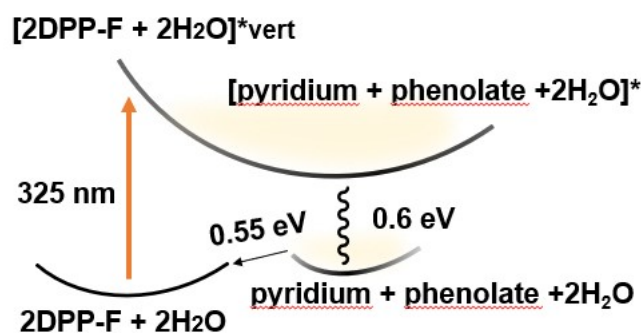


Figure S16. Calculation results from quantum-chemical calculation (see the analysis in detail on part-1 calculation).

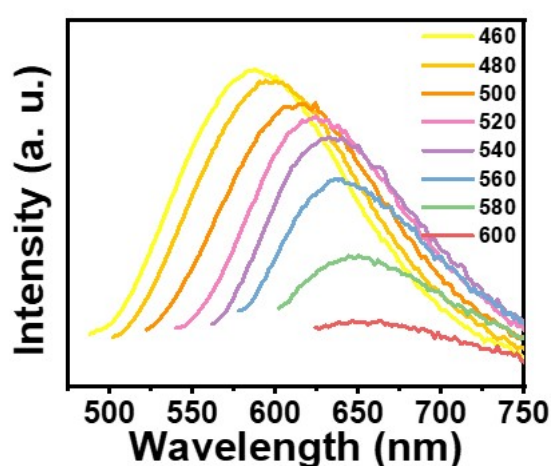


Figure S17. The emission spectra of DPP-F crystal under different excitation wavelength, which could be ascribed to an excitation wavelength-dependent property.

#### 4.Characterization spectra.

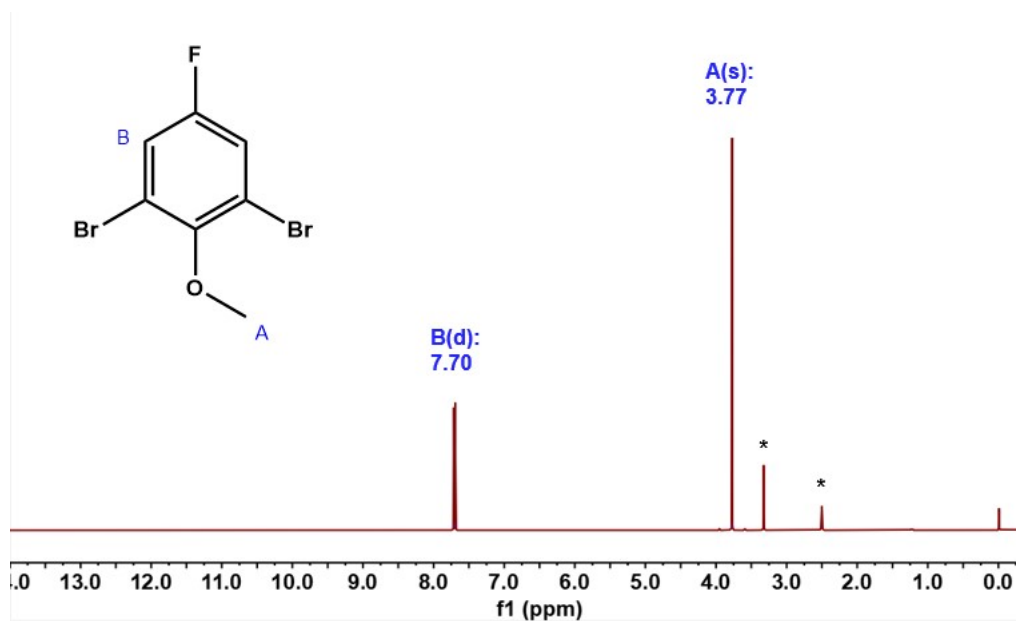


Figure S18. The  $^1\text{H}$  NMR spectrum of 1a.

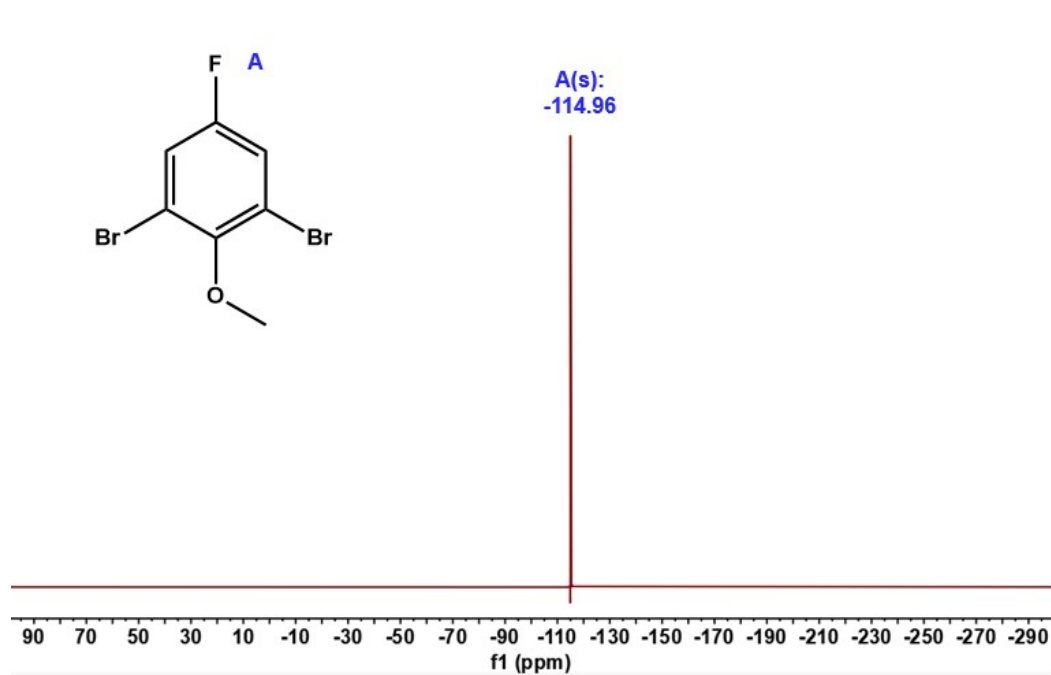


Figure S19. The  $^{19}\text{F}$  NMR spectrum of 1a.



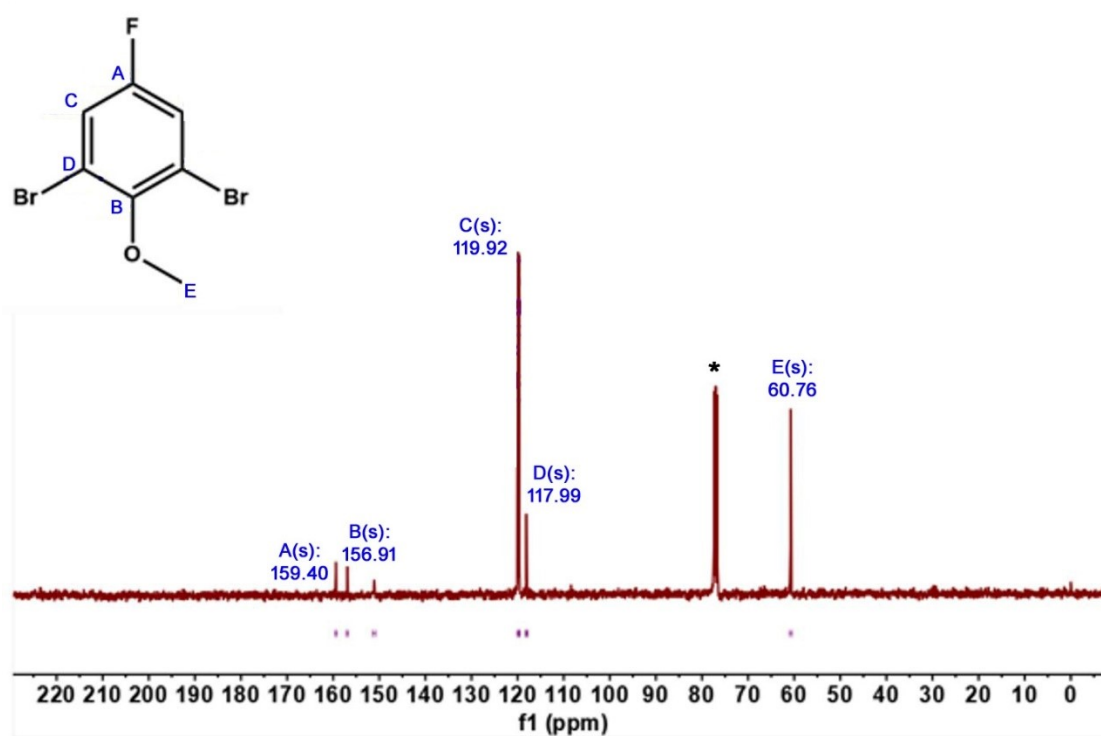


Figure S20. The <sup>13</sup>C NMR spectrum of 1a.

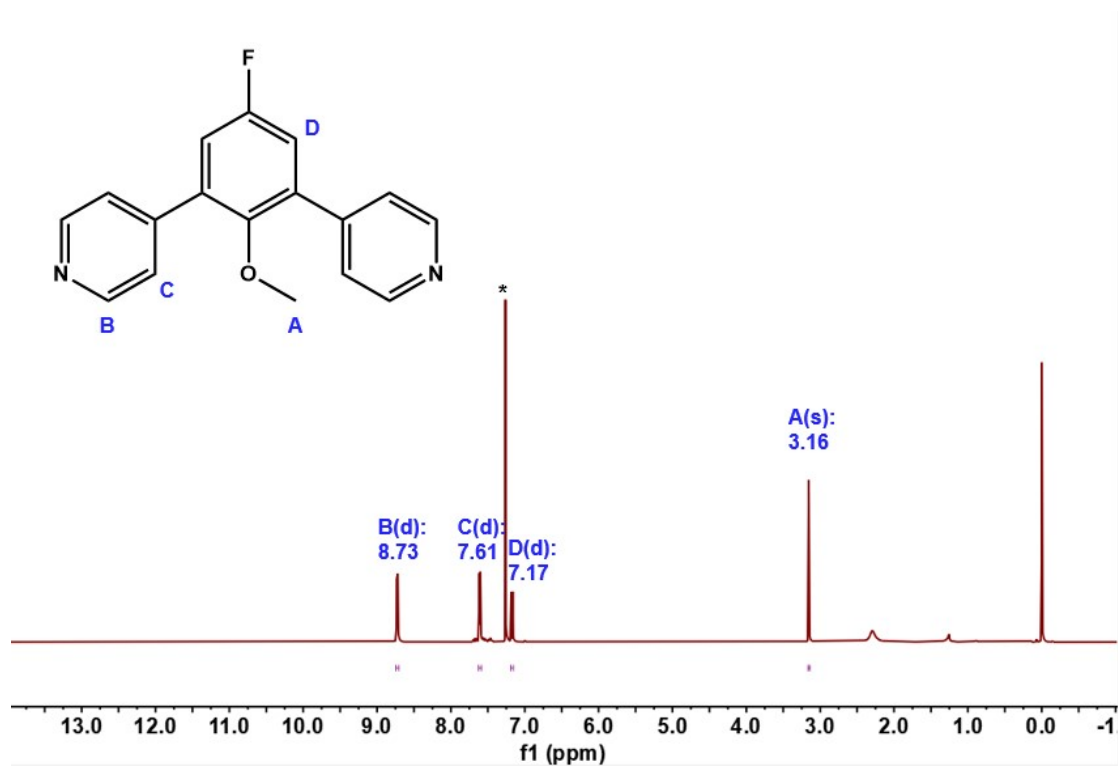


Figure S21. The <sup>1</sup>H NMR spectrum of 1b.

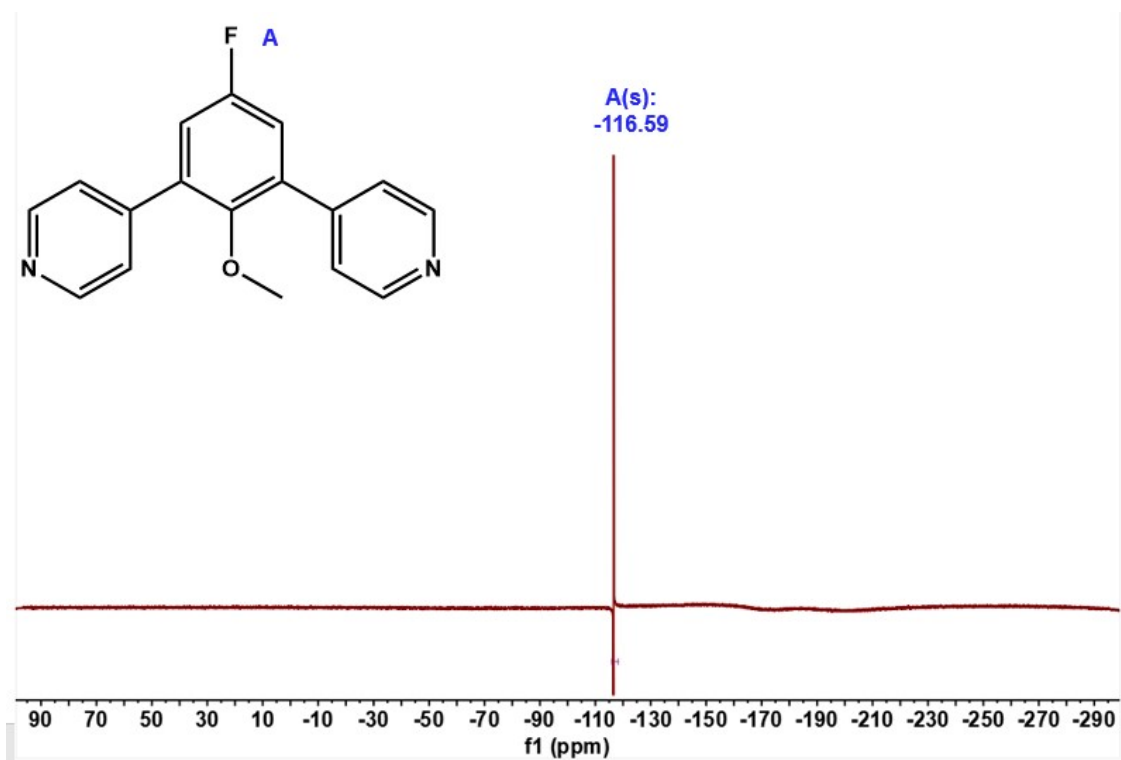


Figure S22. The  $^{19}\text{F}$  NMR spectrum of 1b.

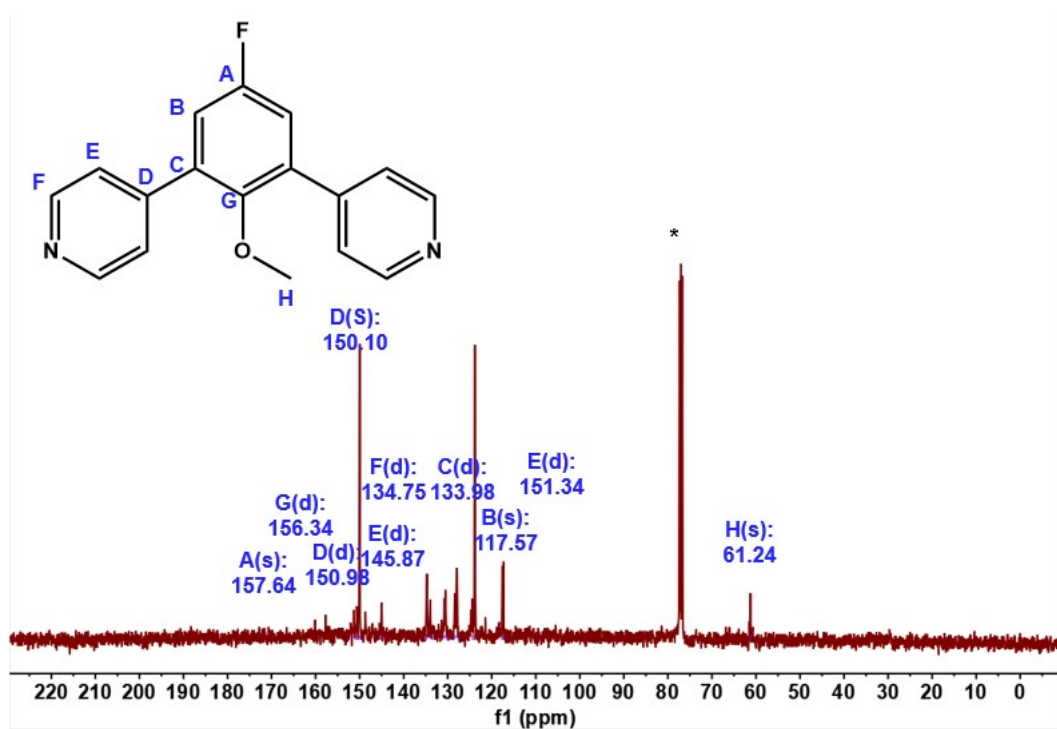


Figure S23. The  $^{13}\text{C}$  NMR spectrum of 1b.

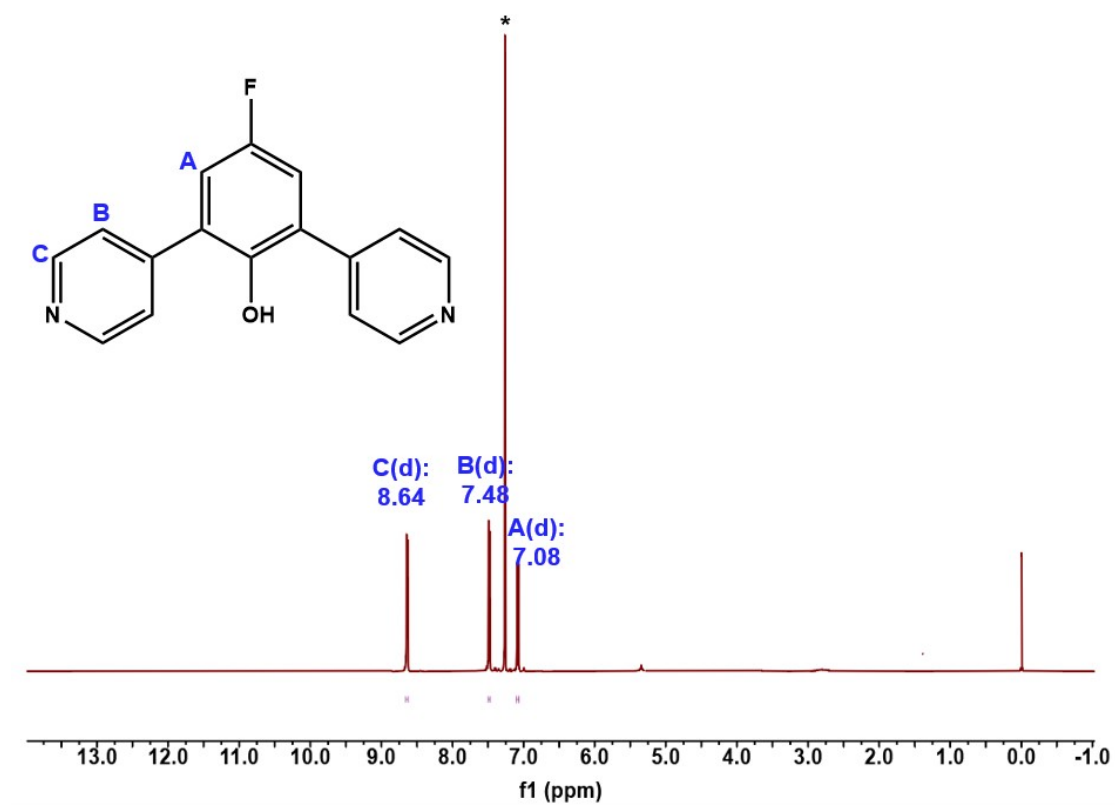


Figure S24. The <sup>1</sup>H NMR spectrum of DPP-F.

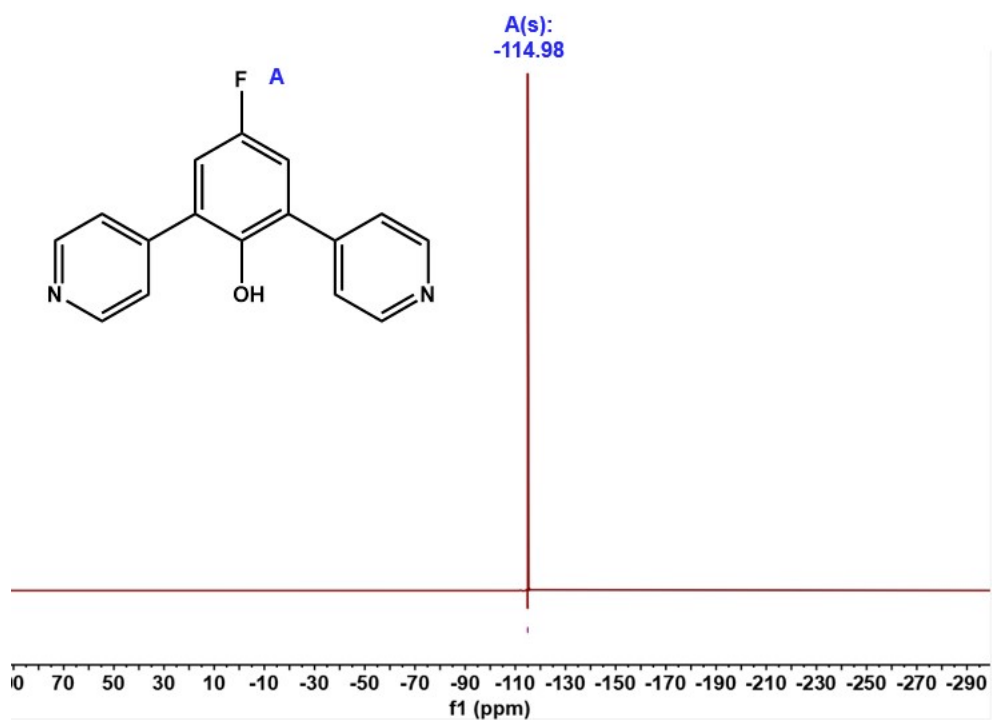


Figure S25. The <sup>19</sup>F NMR spectrum of DPP-F.

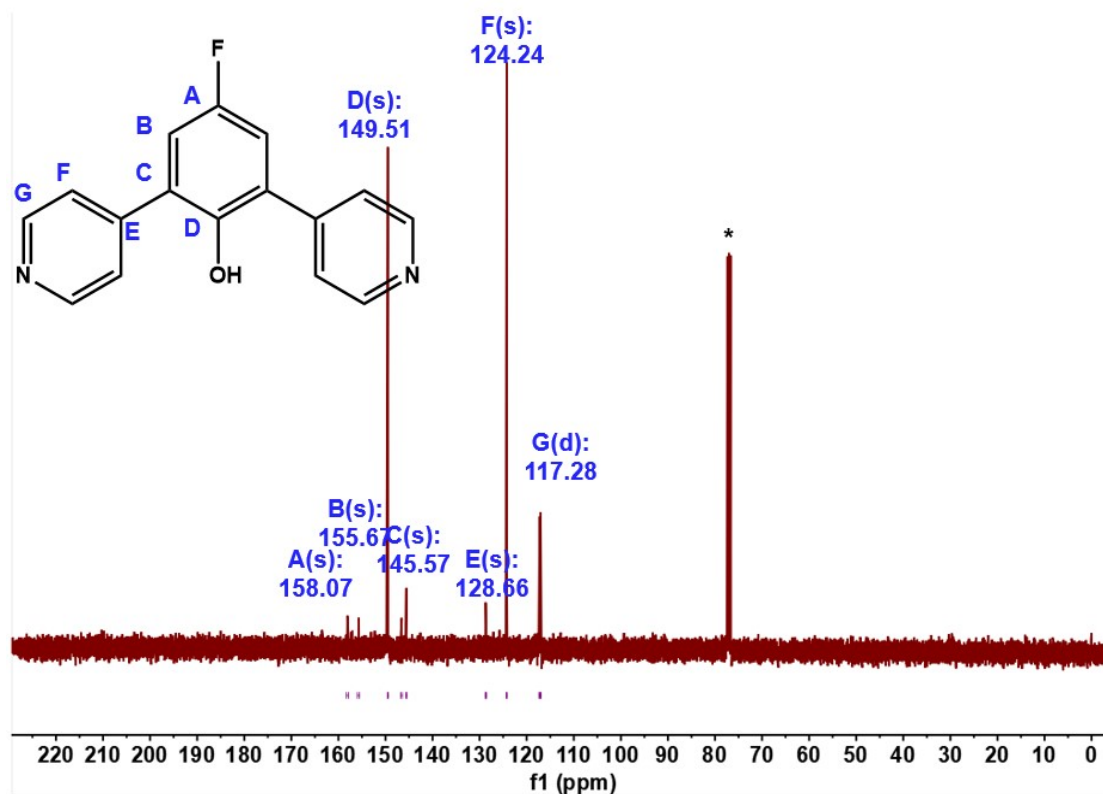


Figure S26. The <sup>13</sup>C NMR spectrum of DPP-F and the predict <sup>13</sup>C NMR spectrum.

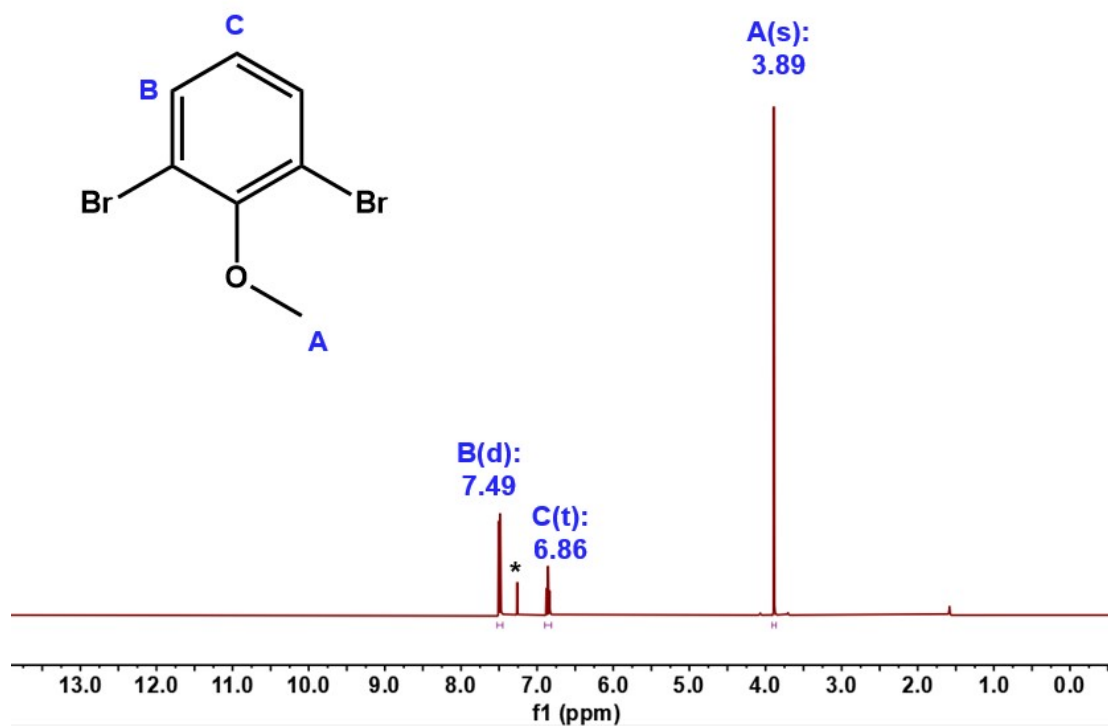


Figure S27. The <sup>1</sup>H NMR spectrum of 2a.

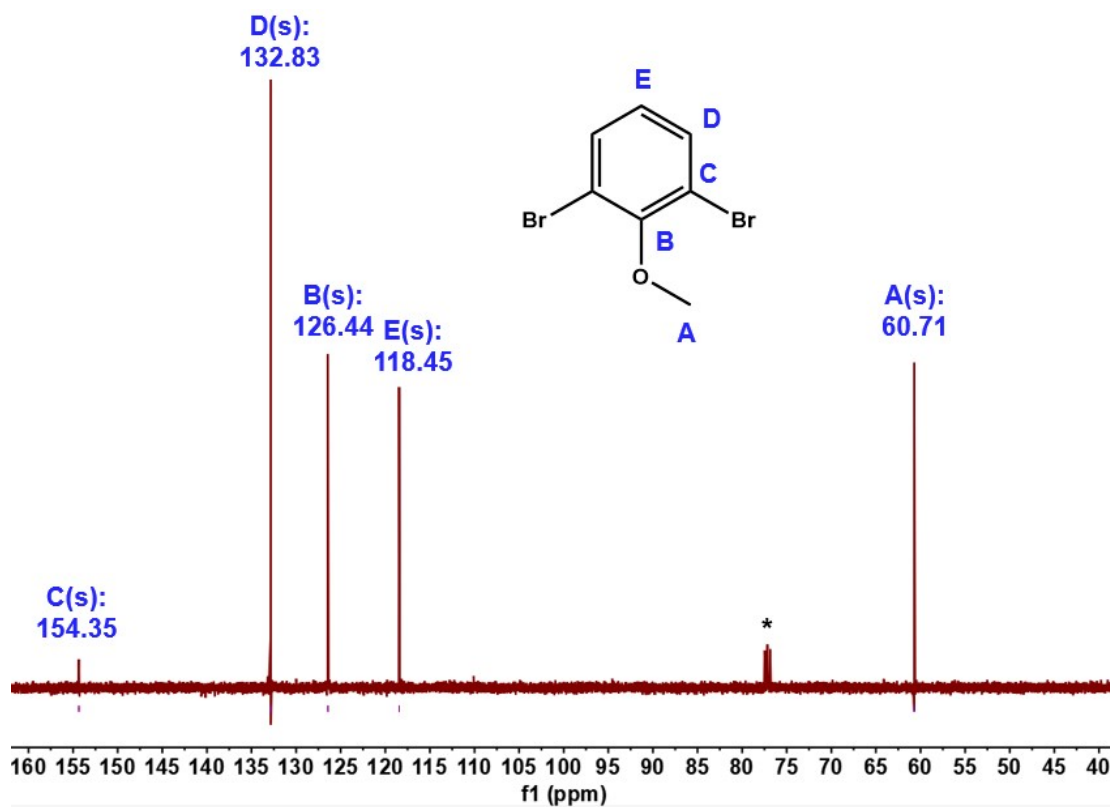


Figure S28. The <sup>13</sup>C NMR spectrum of 2a.

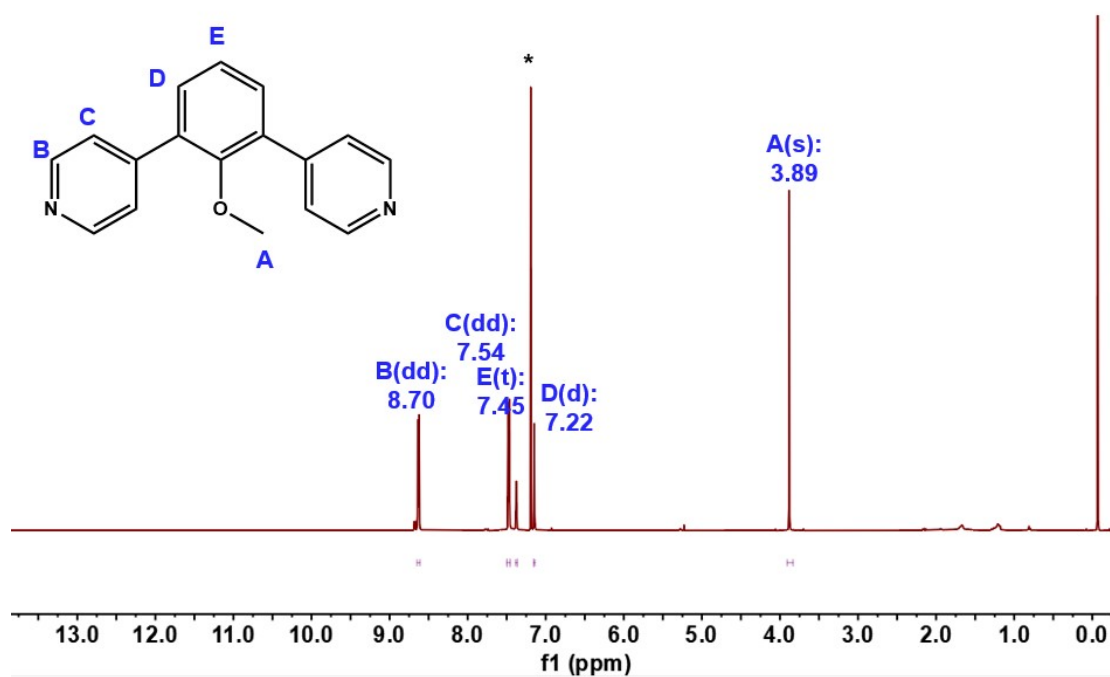


Figure S29. The <sup>1</sup>H NMR spectrum of 2b.

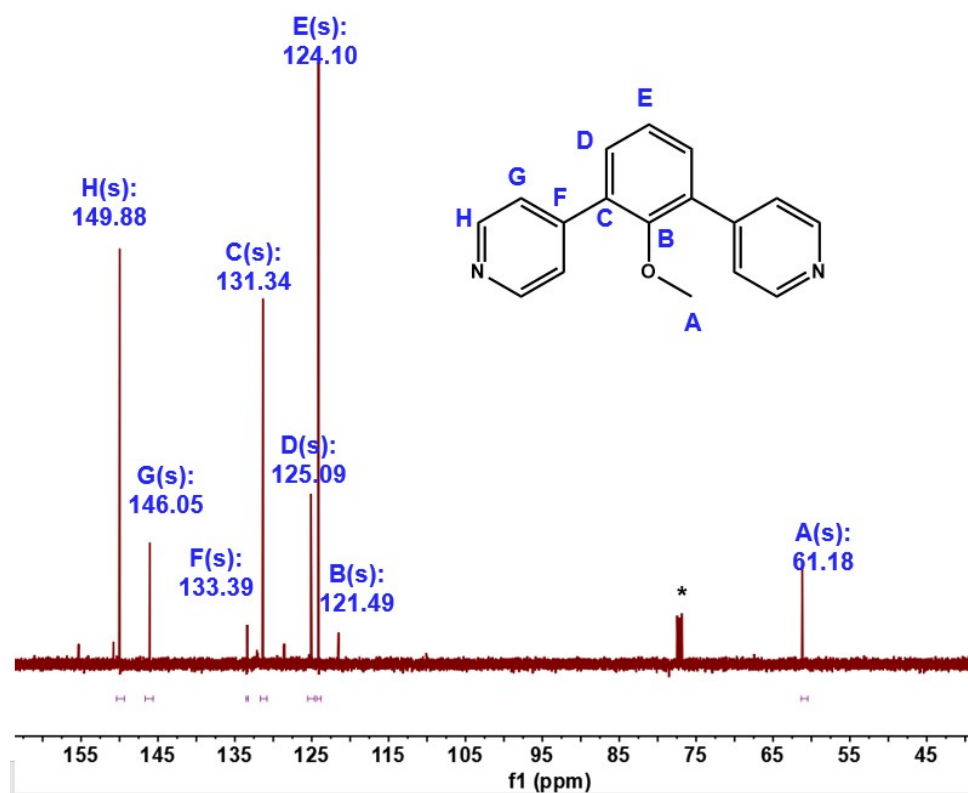


Figure S30. The <sup>13</sup>C NMR spectrum of 2b.

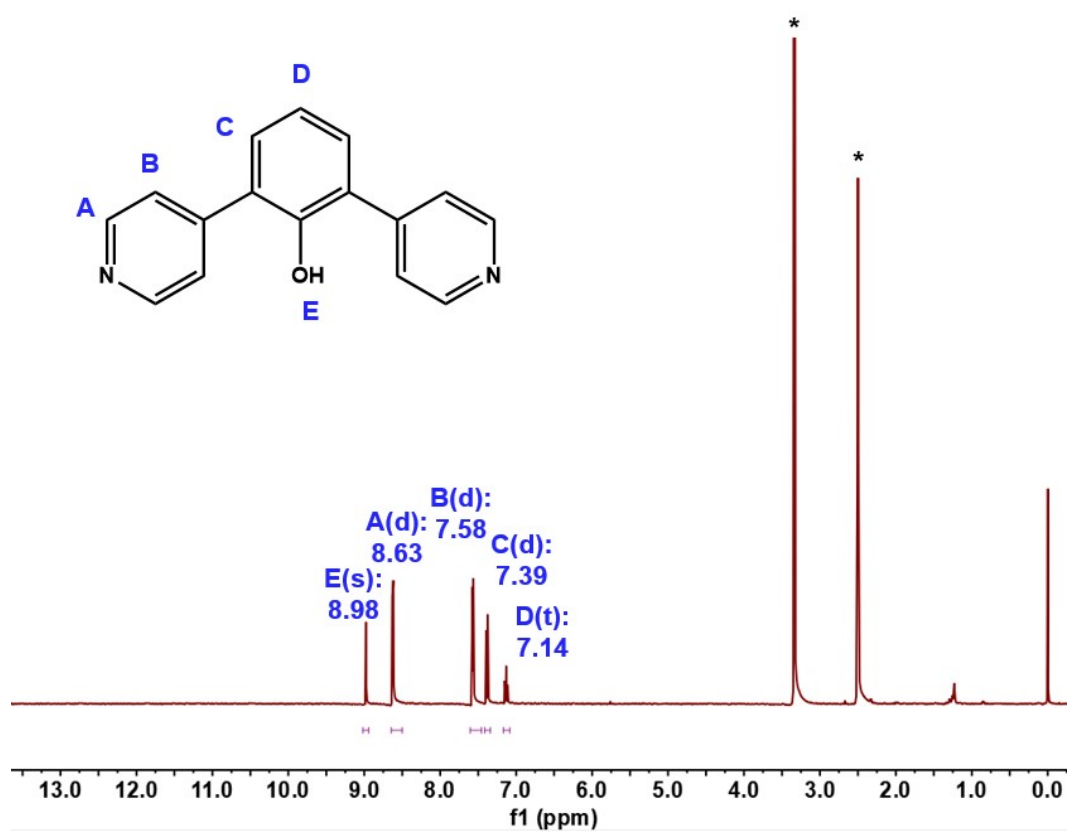


Figure S31. The  $^1\text{H}$  NMR spectrum of DPP.

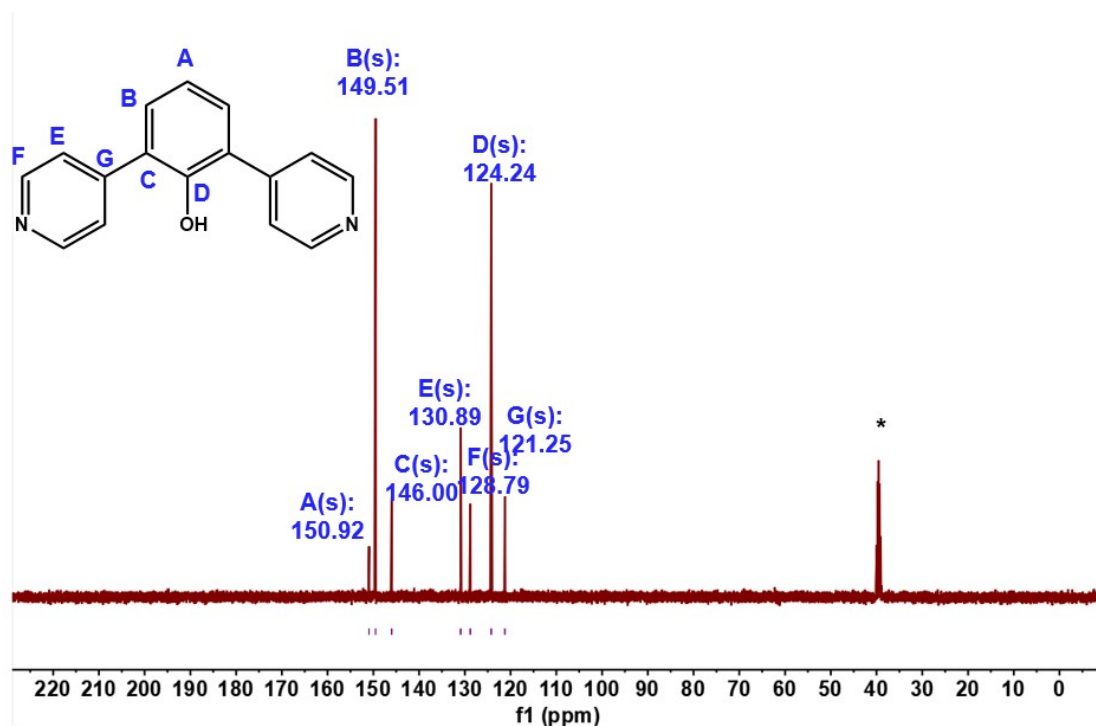


Figure S32. The  $^{13}\text{C}$  NMR spectrum of DPP.

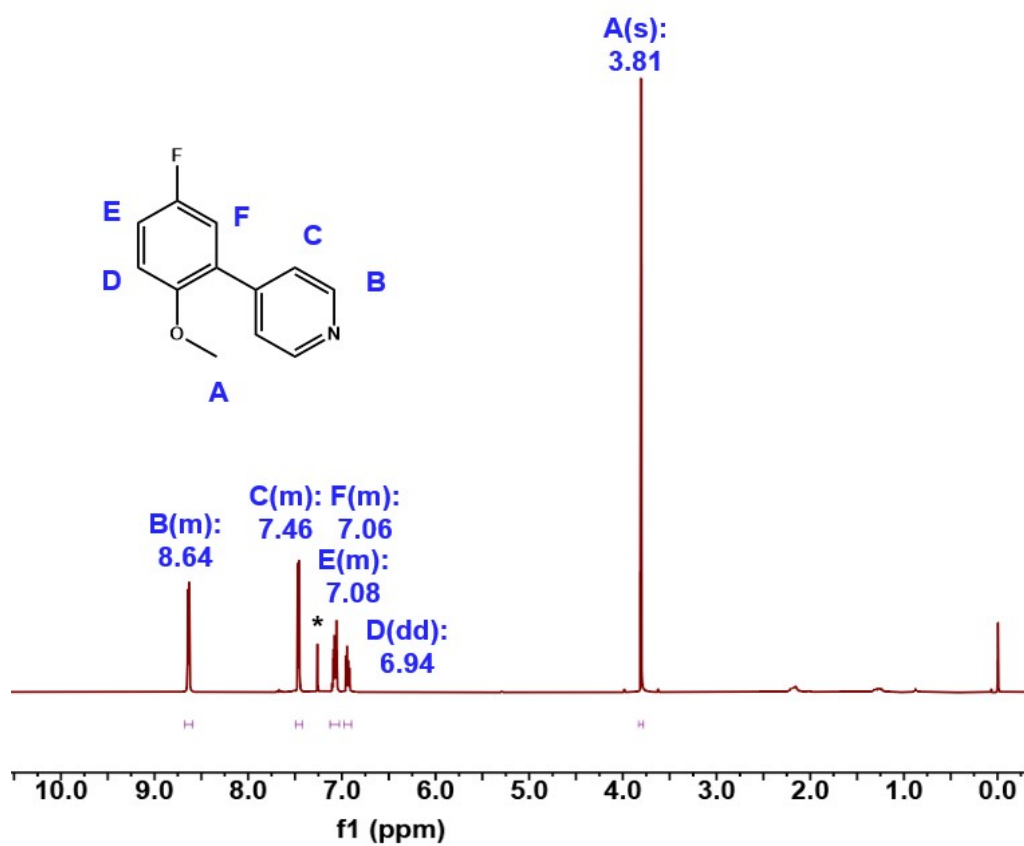


Figure S33. The  $^1\text{H}$  NMR spectrum of 3a.

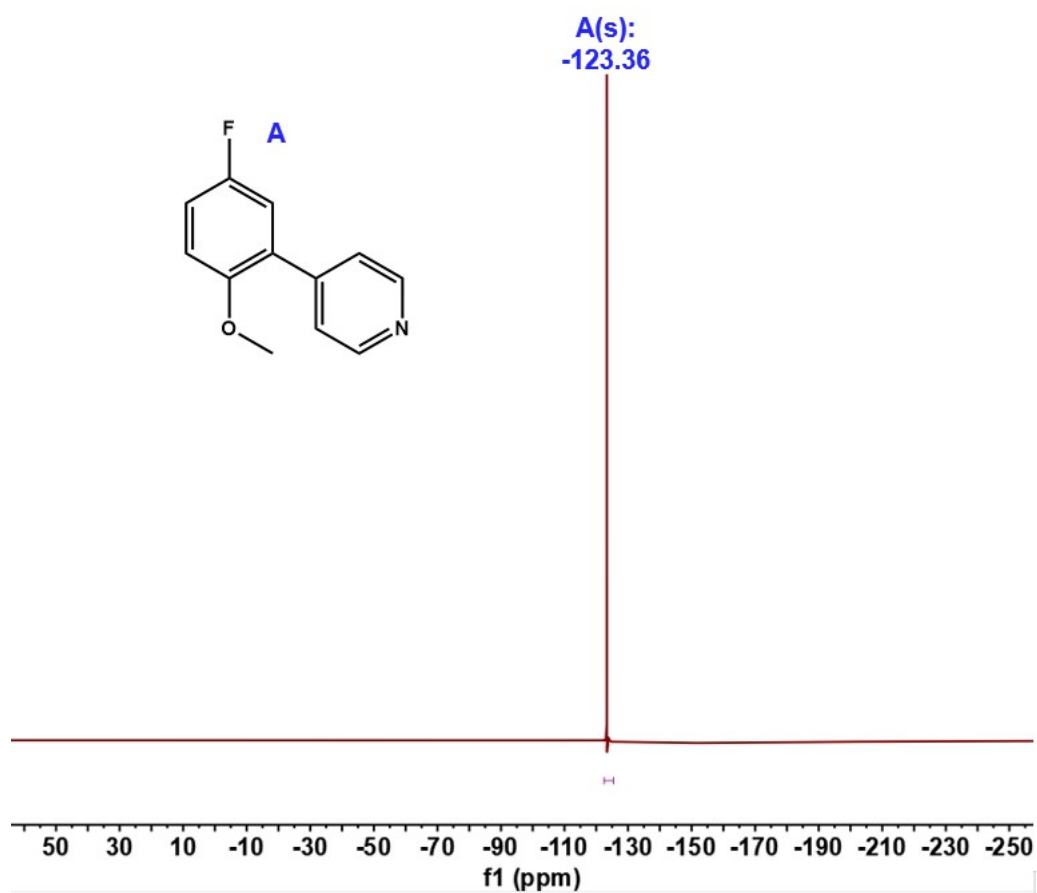


Figure S34. The <sup>19</sup>F NMR spectrum of 3a.

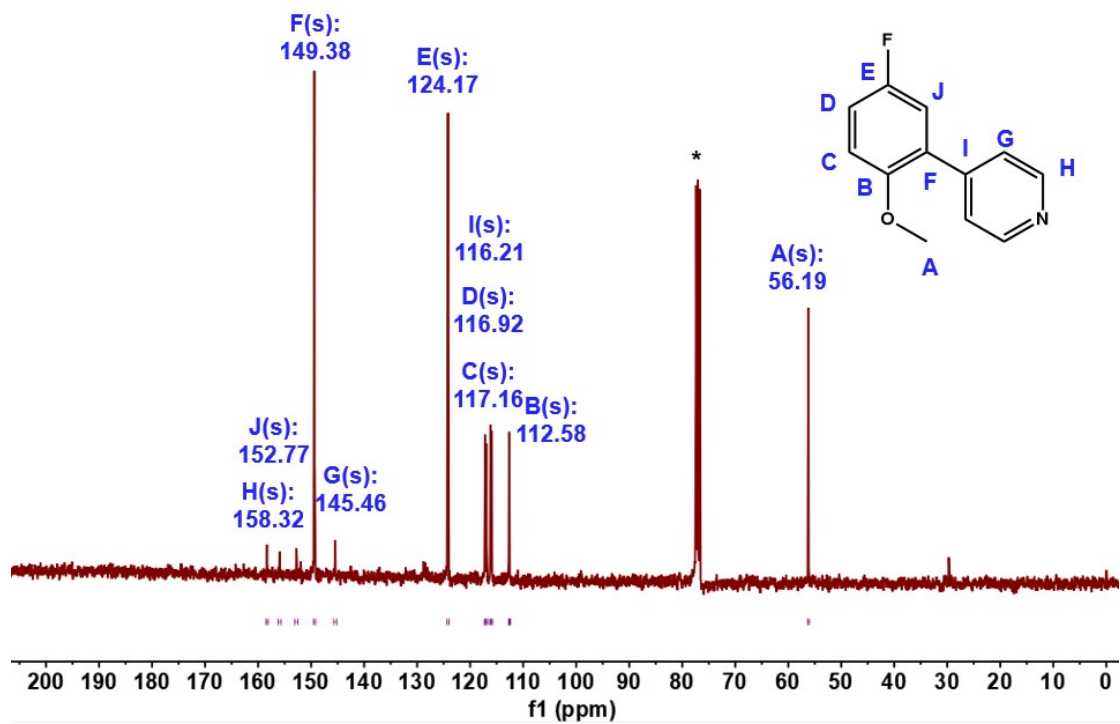


Figure S35. The <sup>13</sup>C NMR spectrum of 3a.



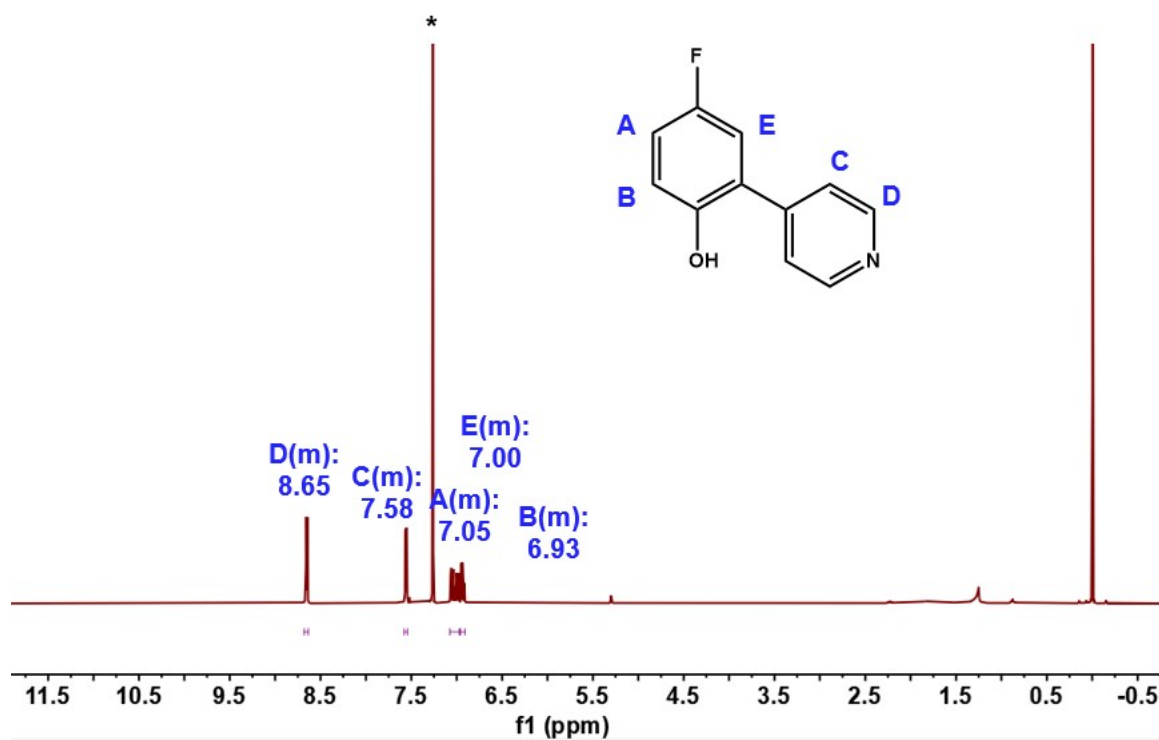


Figure S36. The <sup>1</sup>H NMR spectrum of PP-F.

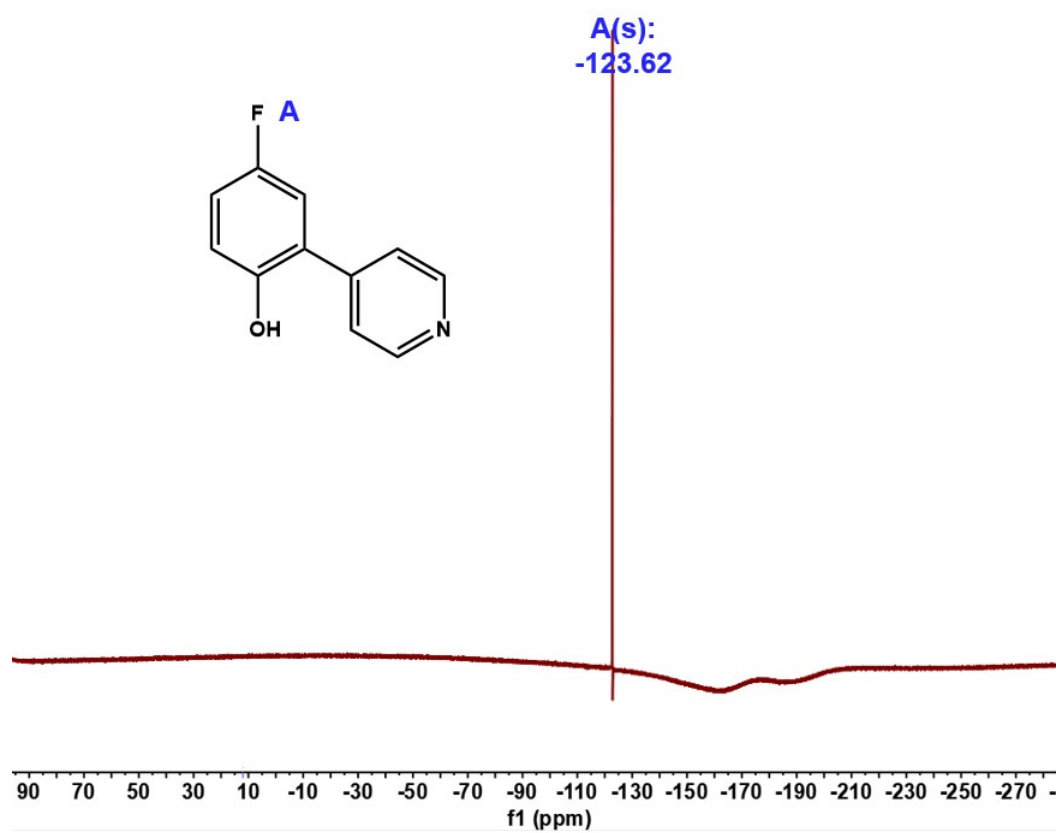


Figure S37. The <sup>19</sup>F NMR spectrum of PP-F.

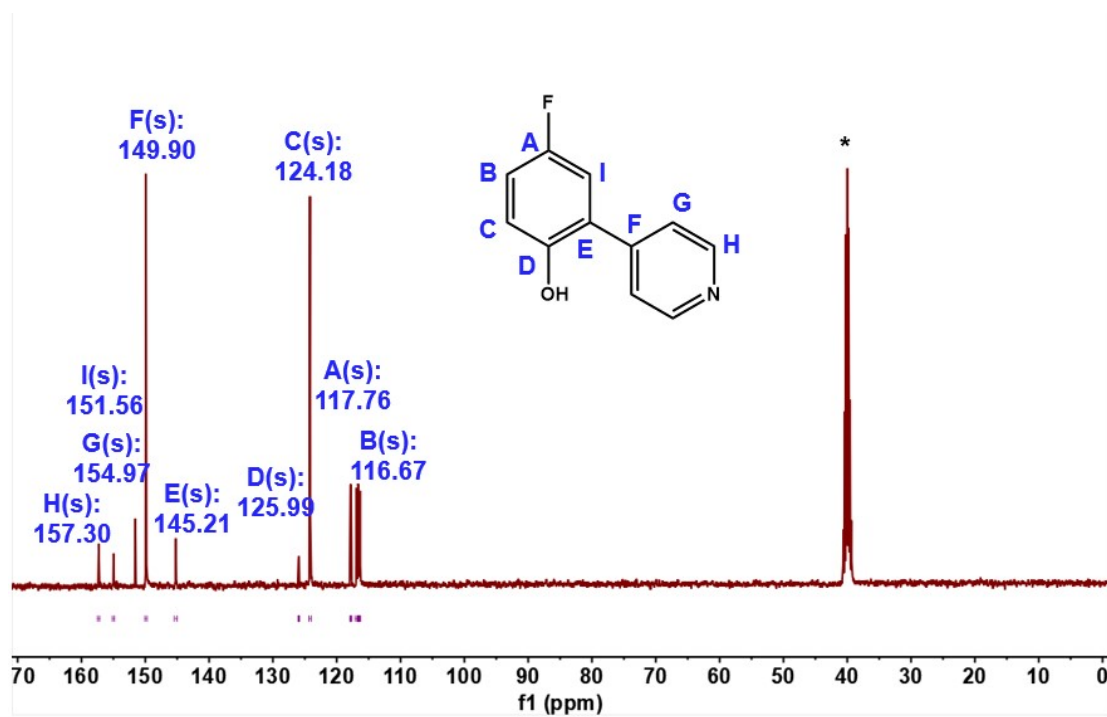


Figure S38. The  $^{13}\text{C}$  NMR spectrum of PP-F.

## 5. Single crystal analysis of compounds

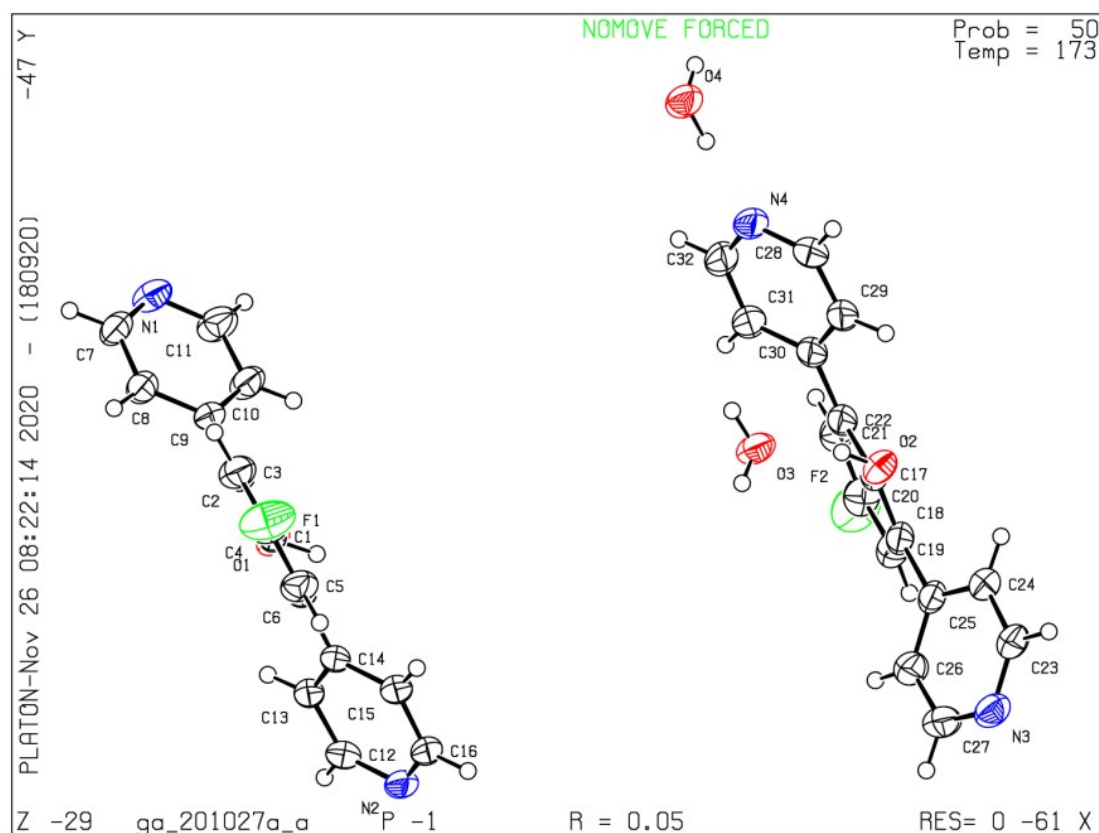


Figure S39. The single crystal structure of DPP-F.

Table S2. Crystal data and refinement details for DPP-F.

Compound	DPP-F
CCDC number	2090476
Empirical formula	C <sub>16</sub> H <sub>13</sub> F N <sub>2</sub> O <sub>2</sub>
Formula weight	284.28
Temperature	173(2) K
Wavelength	1.34138 Å
Crystal system, space group	Triclinic, P-1
Unit cell dimensions	a = 10.5395(10) Å    α = 76.844(4)° b = 10.6712(10) Å    β = 85.075(4)° c = 13.2594(12) Å    γ = 72.914(4)°
Volume	1387.8(2) Å <sup>3</sup>
Z, Calculated density	4, 1.361 Mg/m <sup>3</sup>
Absorption coefficient	0.532 mm <sup>-1</sup>
F(000)	592

Crystal size	0.250 x 0.100 x 0.010 mm <sup>3</sup>
Theta range for data collection	3.818 to 55.499°.
Index ranges	-12<=h<=12, -13<=k<=13, -16<=l<=16
Reflections collected	21600
Independent reflections	5368 [R(int) = 0.0677]
Completeness to theta = 53.594°	99.7 %
Absorption correction	Semi-empirical from equivalents
Max. and min. transmission	0.864 and 0.594
Refinement method	Full-matrix least-squares on F <sup>2</sup>
Data / restraints / parameters	5368 / 0 / 403
Goodness-of-fit on F <sup>2</sup>	1.062
Final R indices [I>2sigma(I)]	R1 = 0.0501, wR2 = 0.1412
R indices (all data)	R1 = 0.0719, wR2 = 0.1536
Extinction coefficient	n/a
Largest diff. peak and hole	0.216 and -0.207 e.Å <sup>-3</sup>

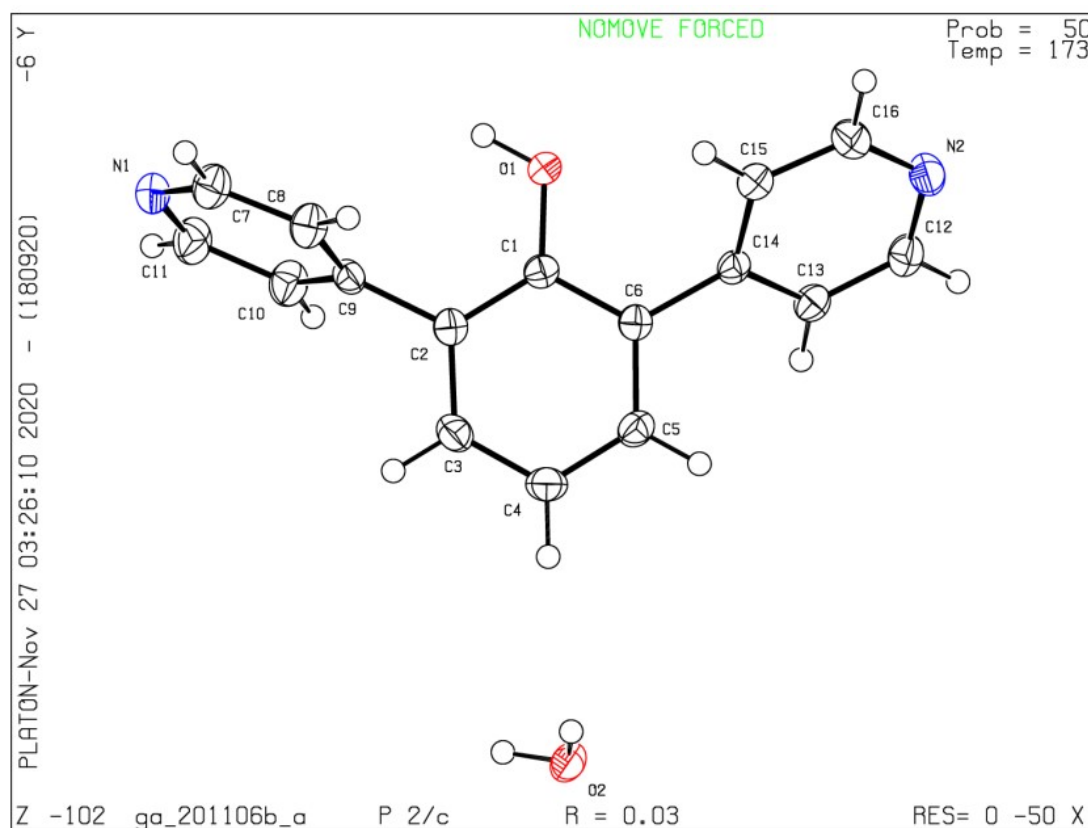


Figure S40. The single crystal structure of DPP.

Table S3. Crystal data and refinement details for DPP.

Compound	DPP
CCDC number	2090477
Empirical formula	C <sub>16</sub> H <sub>14</sub> N <sub>2</sub> O <sub>2</sub>
Formula weight	266.29
Temperature	173(2) K
Wavelength	1.34138 Å
Crystal system, space group	Monoclinic, P2/c
Unit cell dimensions	a = 9.9480(6) Å    α = 90° b = 5.7541(3) Å    β = 100.984(3)° c = 23.8405(14) Å    γ = 90°
Volume	1339.67(13) Å <sup>3</sup>
Z, Calculated density	4, 1.320 Mg/m <sup>3</sup>
Absorption coefficient	0.456 mm <sup>-1</sup>
F(000)	560
Crystal size	0.210 x 0.140 x 0.060 mm <sup>3</sup>
Theta range for data collection	3.286 to 56.494°.
Index ranges	-12 ≤ h ≤ 12, -7 ≤ k ≤ 7, -29 ≤ l ≤ 29
Reflections collected	18175
Independent reflections	2695 [R(int) = 0.0488]
Completeness to theta = 53.594°	99.9 %
Absorption correction	Semi-empirical from equivalents
Max. and min. transmission	0.751 and 0.668
Refinement method	Full-matrix least-squares on F <sup>2</sup>
Data / restraints / parameters	2695 / 0 / 193
Goodness-of-fit on F <sup>2</sup>	1.039
Final R indices [I > 2σ(I)]	R1 = 0.0341, wR2 = 0.0786
R indices (all data)	R1 = 0.0407, wR2 = 0.0828
Extinction coefficient	n/a
Largest diff. peak and hole	0.196 and -0.182 e.Å <sup>-3</sup>

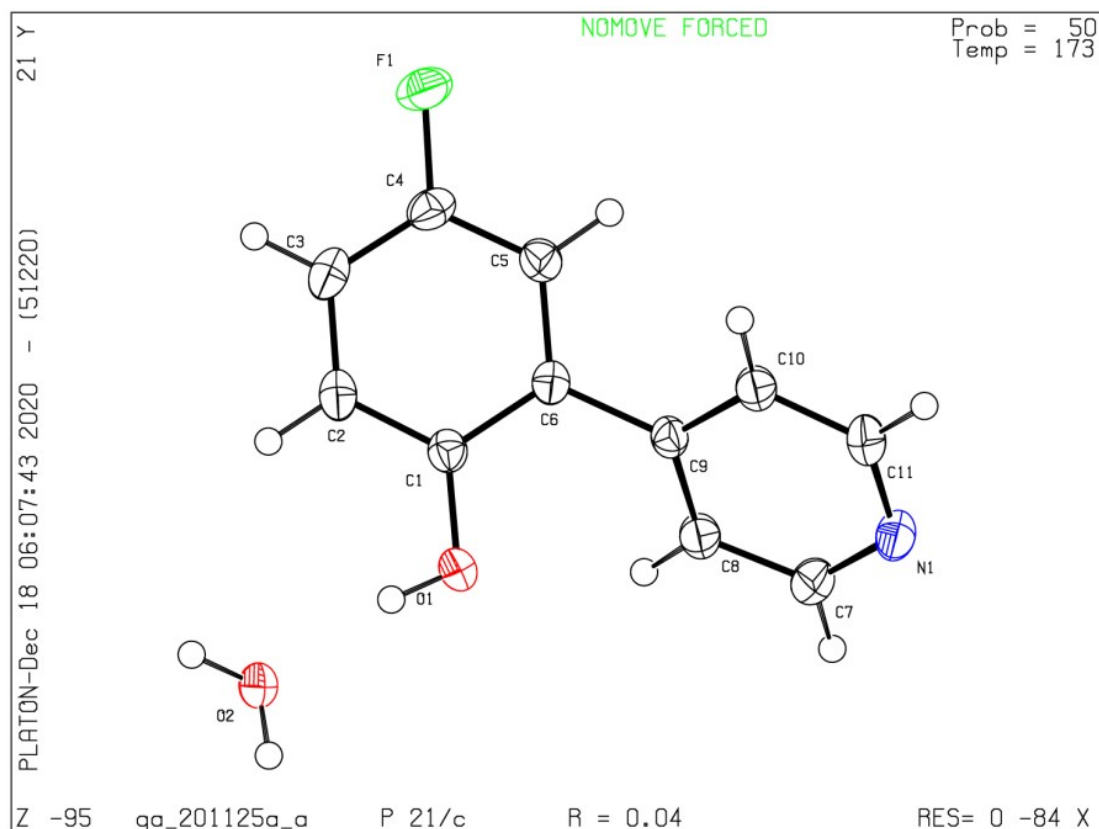


Figure S41. The single crystal structure of DPP.

Table S4. Crystal data and refinement details for PP-F.

Compound	PP-F
CCDC number	2090475
Empirical formula	C <sub>11</sub> H <sub>10</sub> F N O <sub>2</sub>
Formula weight	207.20
Temperature	173(2) K
Wavelength	1.34138 Å
Crystal system, space group	Monoclinic, P2 <sub>1</sub> /c
Unit cell dimensions	a = 13.2434(6) Å    α = 90° b = 3.8259(2) Å    β = 92.630(2)° c = 19.1220(9) Å    γ = 90°
Volume	967.85(8) Å <sup>3</sup>
Z, Calculated density	4, 1.422 Mg/m <sup>3</sup>
Absorption coefficient	0.599 mm <sup>-1</sup>
F(000)	432
Crystal size	0.150 x 0.120 x 0.070 mm <sup>3</sup>
Theta range for data collection	4.027 to 57.995°.
Index ranges	-16 ≤ h ≤ 16, -4 ≤ k ≤ 4, -23 ≤ l ≤ 24
Reflections collected	11220

Independent reflections	2043 [R(int) = 0.0504]
Completeness to theta = 53.594°	99.6 %
Absorption correction	Semi-empirical from equivalents
Max. and min. transmission	0.751 and 0.600
Refinement method	Full-matrix least-squares on F <sup>2</sup>
Data / restraints / parameters	2043 / 0 / 148
Goodness-of-fit on F <sup>2</sup>	1.054
Final R indices [I>2sigma(I)]	R1 = 0.0379, wR2 = 0.1055
R indices (all data)	R1 = 0.0413, wR2 = 0.1095
Extinction coefficient	n/a
Largest diff. peak and hole	0.266 d -0.223 e.Å <sup>-3</sup>

---

## 6.Reference

- [1] (a) C. Lee, W. Yang, R. G. Parr, *Physical Review B* **1988**, 37, 785-789; (b) A. D. Becke, *J. Chem. Phys.* **1993**, 98, 5648-5652.
- [2] (a) M. J. Frisch, J. A. Pople, J. S. Binkley, *J. Chem. Phys.* **1984**, 80, 3265-3269; (b) R. Ditchfield, W. J. Hehre, J. A. Pople, *J. Chem. Phys.* **1971**, 54, 724-728; (c) T. Clark, J. Chandrasekhar, G. W. Spitznagel, P. V. R. Schleyer, *J. Comput. Chem.* **1983**, 4, 294-301.
- [3] S. Grimme, J. Antony, S. Ehrlich, H. Krieg, *J. Chem. Phys.* **2010**, 132, 154104.
- [4] (a) R. Bauernschmitt, R. Ahlrichs, *Chem. Phys. Lett.* **1996**, 256, 454-464; (b) F. Furche, R. Ahlrichs, *J. Chem. Phys.* **2002**, 117, 7433-7447.
- [5] S. Miertuš, E. Scrocco, J. Tomasi, *Chem. Phys.* **1981**, 55, 117-129.